

Review

Cell-Adhesion Properties of β -Subunits in the Regulation of Cardiomyocyte Sodium Channels

Samantha C. Salvage ^{1,*} , Christopher L.-H. Huang ^{1,2} and Antony P. Jackson ^{1,*} ¹ Department of Biochemistry, University of Cambridge, Cambridge CB2 1QW, UK; clh11@cam.ac.uk² Department of Physiology, Development and Neuroscience, University of Cambridge, Cambridge CB2 3EG, UK

* Correspondence: ss2148@cam.ac.uk (S.C.S.); apj10@cam.ac.uk (A.P.J.); Tel.: +44-1223-765950 (S.C.S.); +44-1223-765951 (A.P.J.)

Received: 7 June 2020; Accepted: 27 June 2020; Published: 1 July 2020



Abstract: Voltage-gated sodium (Nav) channels drive the rising phase of the action potential, essential for electrical signalling in nerves and muscles. The Nav channel α -subunit contains the ion-selective pore. In the cardiomyocyte, Nav1.5 is the main Nav channel α -subunit isoform, with a smaller expression of neuronal Nav channels. Four distinct regulatory β -subunits (β 1–4) bind to the Nav channel α -subunits. Previous work has emphasised the β -subunits as direct Nav channel gating modulators. However, there is now increasing appreciation of additional roles played by these subunits. In this review, we focus on β -subunits as homophilic and heterophilic cell-adhesion molecules and the implications for cardiomyocyte function. Based on recent cryogenic electron microscopy (cryo-EM) data, we suggest that the β -subunits interact with Nav1.5 in a different way from their binding to other Nav channel isoforms. We believe this feature may facilitate *trans*-cell-adhesion between β 1-associated Nav1.5 subunits on the intercalated disc and promote ephaptic conduction between cardiomyocytes.

Keywords: voltage-gated sodium (Nav) channels; Nav1.5; sodium (Nav) channel β -subunits; cell-adhesion; ephaptic conduction

1. Introduction

Cardiomyocytes within cardiac muscle bundles perform the involuntary contraction and relaxation cycle that is the cellular basis of the heartbeat. Cardiomyocytes possess unique adaptations to ensure this process is tightly synchronised between individual cells. In particular, the cardiomyocytes are both physically and electrically connected to each other via their intercalated discs. On the lateral membrane, T-tubules facilitate the transmission of the electrical signal from the cell surface, to deeper within the cell. This stimulates the release of calcium from the sarcoplasmic reticulum and the initiation of sarcomere contraction (Figure 1) [1].

The cardiac action potential underlies electrical signalling and is initiated by the transient depolarisation of voltage-gated sodium (Nav) channels (for further details, see Ref. [2], this volume). The Nav channel α -subunit (Mwt ~220–250 kDa) contains the ion-selective pore. In the human genome, there are nine different functional Nav channel α -subunit genes encoding proteins Nav1.1–1.9. Different Nav channel α -subunit isoforms are expressed in a tissue-specific manner and exhibit distinct gating behaviour, presumably tailored to their physiological context. In the cardiomyocyte, Nav channels with different gating properties can also be correlated with their differing sub-cellular localisation. The major Nav channel isoform expressed in the heart is Nav1.5. It is mainly localised at the intercalated disc and within caveolae on the sarcolemmal lateral membrane [3]. Cardiomyocytes also express smaller amounts of the neuronal channels Nav1.1, Nav1.3 and Nav1.6, which are predominantly

localised in the T-tubules [4,5]. This pattern is striking and is likely to be functionally significant. For example, on a given cardiomyocyte, all Nav channels will experience the same resting potential. However, Nav1.5 activates at more negative potentials and more slowly compared to neuronal Nav channels. Thus, Nav1.5 at the intercalated disc and on the sarcolemma may initiate the cardiac action potential as it propagates from one cardiomyocyte to another within the muscle fibre [5,6]. By contrast, a delayed T-tubular excitation of the neuronal Nav channels will be matched by their more negative threshold for excitation and the more rapid kinetics of activation. This, combined with the close structural association between the neuronal Nav channels, the sodium-calcium exchanger (NCX) and the voltage-gated calcium channels on the T-tubular membrane and with the ryanodine receptors (RyR) on the adjacent sarcoplasmic reticulum, permits T-tubular activation that is synchronous with the surface action potential and that optimally initiates excitation-contraction coupling [4,7].

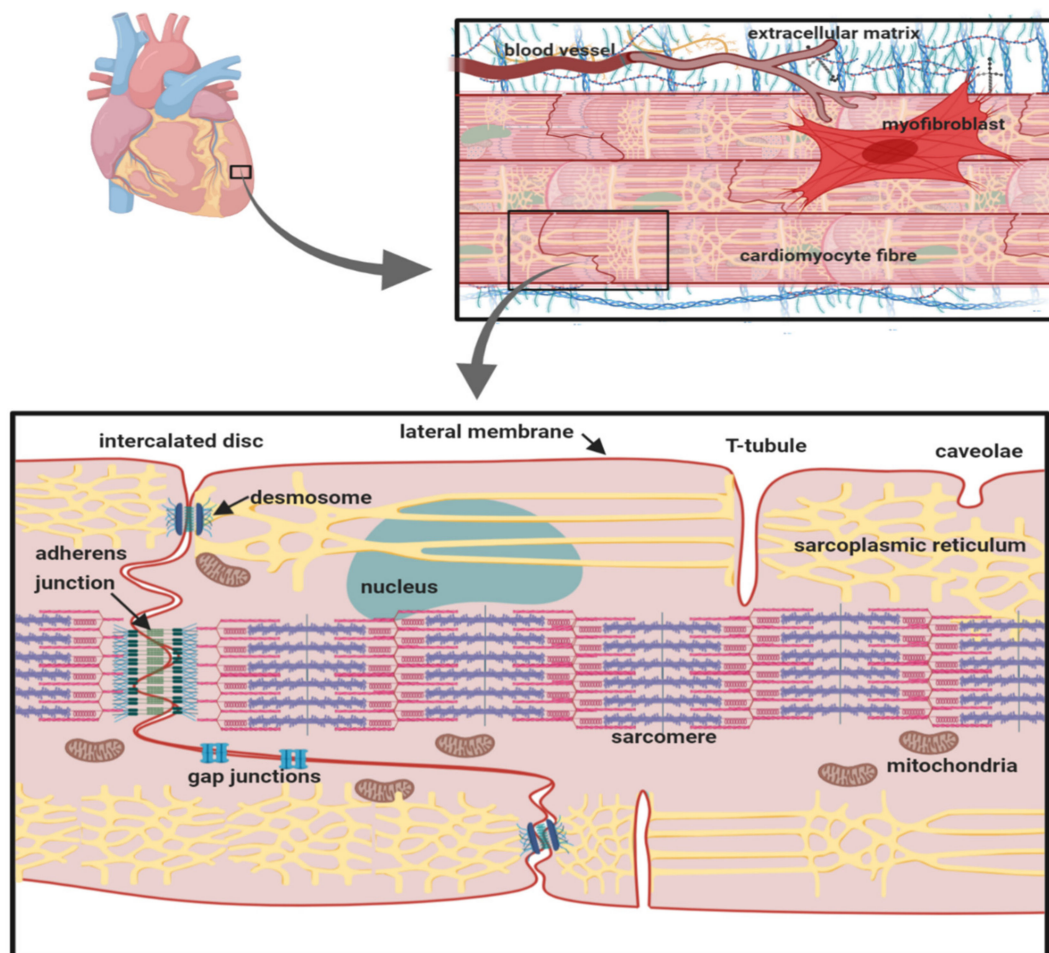


Figure 1. The cardiomyocyte: its anatomical and cellular context. The location of key organelles, membrane compartments and molecular components mentioned in the text are indicated.

1.1. The Nav Channel α -Subunit

All Nav channel α -subunits contain four internally homologous domains (DI–IV). Each domain contains six transmembrane α helices (S1–S6) (Figure 2A). Helix S4 of each domain contains positively charged amino acid residues along one face of the helix. The movement of the S4 helices in response to changes in membrane potential is transmitted to helices S5 and S6 of each domain. This leads to the transient opening and subsequent inactivation of the channel pore [8,9]. High-resolution structures obtained by cryogenic electron microscopy (cryo-EM), for the heart-specific Nav1.5 α -subunit, the skeletal muscle channel Nav1.4 and the neuronal channels Nav1.2 and Nav1.7

show that the four domains surround the central pore with four-fold pseudosymmetry. Helices S1–S4 lie on the outer rim of the channel, with helices S5 and S6 from each domain forming the channel pore region [10–14]. This topology is highly conserved between Nav α -subunit isoforms, as illustrated by comparison of the Nav1.7 and Nav1.5 structures (Figure 2B).

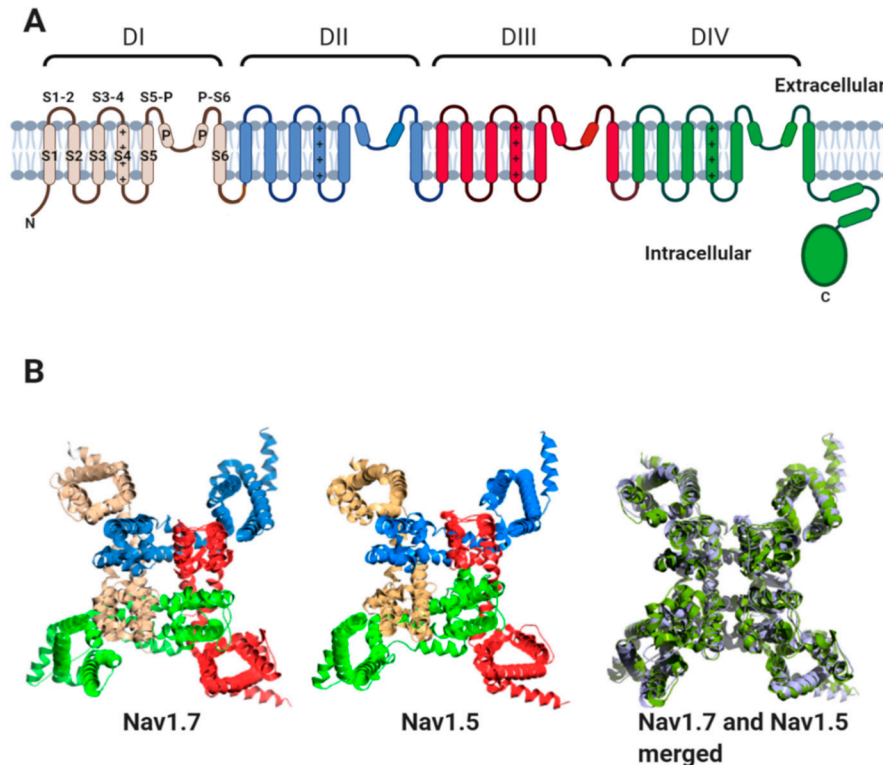


Figure 2. The Nav channel α -subunit. (A) Cartoon representation showing internally homologous domains DI–DIV. In DI, the location of transmembrane alpha-helices, S1–S6, the extracellular loops (S1-2; S3-4; S5-P and P-S6) and the re-entrant P helices are indicated. The positive charges on the S4 helices of each domain are indicated. (B) Three-dimensional structures of human Nav1.7 (PDB: 6JH8I), rat Nav1.5 (PDB: 6UZ3), and their aligned structures. The channels are viewed from above the plane of the plasma membrane. For Nav1.5 and Nav1.7, the domains DI–DIV are coloured as in (A). For aligned structures, Nav1.7 is coloured blue–white and Nav1.5 is coloured pale green.

1.2. The Nav Channel β -Subunits and Their Binding Sites on the α -Subunits

Vertebrate Nav channels are typically associated with one or more β -subunits (Mwt ~30–40 kDa). There are four homologous β -subunit genes (*SCN1b-4b*) encoding subunit proteins β 1– β 4 respectively. The β -subunits are type I transmembrane proteins consisting of a single extracellular N-terminal V-type immunoglobulin (Ig) domain, connected to a transmembrane alpha-helix by a flexible neck and terminating in a largely disordered intracellular C-terminal region (Figure 3A,B). An alternatively spliced form of β 1, known as β 1B, is also expressed in the heart. It consists of an Ig domain identical to that of β 1, but lacks the transmembrane alpha-helix and is therefore secreted (Figure 3A) [15]. The β 1- and β 3-subunits show the closest sequence similarity to each other and are more distantly related to β 2 and β 4 (Figure 3C) [16,17]. The β -subunits have multiple effects on Nav channel gating behaviour that vary between individual β -subunit isoforms. In general terms however, they can increase the peak current density of Nav channels, probably by enhancing trafficking to the plasma membrane [2]. They also shift the voltage ranges over which Nav channel steady-state activation and/or inactivation occur, and in some cases enhance the rates of inactivation and recovery from inactivation [18]. As an illustrative example, the β 3-subunit shifts the $V_{1/2}$ for inactivation of Nav1.5 in a depolarising direction: i.e., the voltage at which half the channels are inactivated is displaced to a

more positive value compared to the α -subunit alone (Figure 3D) [19–22]. For a cardiomyocyte with a resting potential of about -90 mV [2], this would act to increase the fraction of functional Nav1.5 channels available in the membrane [17].

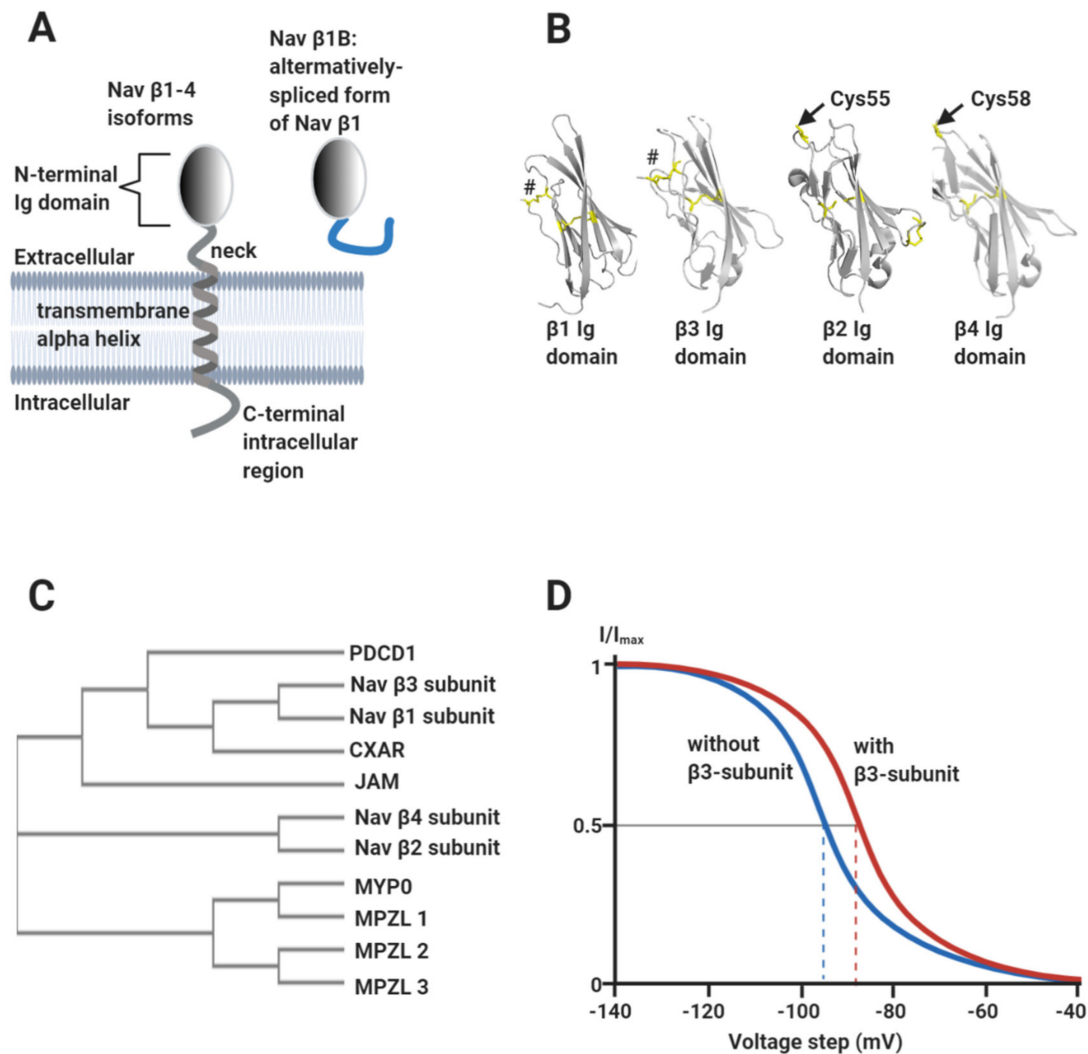


Figure 3. The Nav channel β -subunits. (A) Cartoon showing the common structural features of the β -subunits, including the alternatively spliced β 1B isoform. (B) Atomic-resolution structures for the Ig domains of: β 1 (PDB: 6JHI); β 2, (PDB: 5FEB); β 3 (PDB: 4L1D) and β 4 (PDB: 5XAX). The separate disulphide bonds stabilising the N-terminal strands of β 1 and β 3 are labelled by hashtags and the free, exposed Cys residue on β 2 (Cys55) and β 4 (Cys58) are as indicated. (C) Phylogenetic analysis of Nav channel β -subunits, showing their relationship to members of the Ig domain-containing CAM protein family. PDCD1: programmed cell death protein 1 (<https://www.uniprot.org/uniprot/Q15116>); CXAR: Coxsackievirus and adenovirus receptor (<https://www.uniprot.org/uniprot/P78310>); JAM: junctional adhesion molecule 2 (<https://www.uniprot.org/uniprot/P57087>); MYP0: myelin protein P0 (<https://www.uniprot.org/uniprot/P25189>); MPZL1: myelin protein zero-like protein (<https://www.uniprot.org/uniprot/O95297>); MPZL2: myelin protein zero-like protein 2 (<https://www.uniprot.org/uniprot/O60487>) and MPZL3: myelin protein zero-like protein 3 (<https://www.uniprot.org/uniprot/Q6UWV2>). The phylogenetic tree was constructed using the ClustalW2 package (https://www.ebi.ac.uk/Tools/phylogeny/simple_phylogeny/). (D) Idealised inactivation curves of the Nav1.5 channel in the absence (blue) and the presence (red) of the β 3-subunit. The β 3-subunit induces a depolarising (rightward) shift of the $V_{1/2}$ of inactivation, as indicated on the diagram by the dotted lines.

The β 1-subunit interaction site has been resolved at high resolution for Nav1.2, Nav1.4 and Nav1.7 α -subunits [10–13] and is illustrated for the case of Nav1.7 in Figure 4A,B. The β 1-subunit Ig domain makes ionic and hydrogen-bond contacts with the DI, S5-P extracellular loop, the DIII, S1–S2 extracellular loop and the DIV, P-S6 extracellular loop regions (Figures 2 and 4B). Surprisingly however, the Nav1.5 α -subunit structure has revealed some localised, but structurally significant differences between Nav1.5 and the other studied Nav channels [14]. In particular, the Nav1.7 Glu307 residue in the DI, S5-P extracellular loop, is changed in Nav1.5 to an asparagine residue, Asn319. This creates an N-linked glycosylation site that is not present in any other Nav channel isoform. In the Nav1.5 cryo-EM structure, there is electron density around Asn319 that is consistent with a complex N-linked glycan (Figure 4C). It should be noted that the electron density detected in the cryo-EM data only corresponds with two N-acetyl glucosamine residues of the core glycan. The remaining, diverse sugar moieties of the terminal branches are not resolved, presumably due to their inherent flexibility. Thus the N-linked glycan attached to Nav1.5, Asn319 extends further than the resolved electron density and would certainly be bulky enough to occlude the binding site for the β 1 Ig domain [12]. Moreover, the specific orientation of a second N-linked glycan attached to Nav1.5 residue Asn1390 will probably also interfere with the binding of the β 1 Ig domain (Figure 4C). Hence, it seems likely that in vivo, although β 1 may still be associated with the Nav1.5 DIII voltage sensing domain via its transmembrane alpha-helix, its Ig domain will not be able to bind to the Nav1.5 α -subunit.

Based on biochemical and electrophysiological data, it is probable that the β 3-subunit transmembrane alpha-helix also binds to Nav1.5 DIII voltage sensing domain [19–21]. Yet, there is evidence that it may bind closer to Nav1.5 DIII helix S3 rather than to the binding site for the β 1 transmembrane region on the DIII helix S2 [19,21]. If so, then a given Nav1.5 α -subunit may be able to bind simultaneously to β 1 and β 3-subunits and there is indeed electrophysiological evidence to support this idea [21,23].

In contrast to β 1 and β 3, which bind to the α -subunit non-covalently, the β 2-subunit binds to Nav1.7 covalently via a disulphide bond between a cysteine on the Ig domain (Cys55) and a corresponding cysteine (Cys895) on the α -subunit DII S5-P extracellular loop (Figure 4D) [12,24]. Neither the transmembrane alpha-helix nor the intracellular region of β 2 is resolved in the published structure, indicating that both must be unconstrained in this purified complex [12]. As with β 2, the β 4-subunit Ig domain also contains a cysteine (Cys58) that can form a disulphide bond to the free cysteine on the α -subunit DII, S5-P site [25]. It is therefore presumed that the β 2 and β 4-subunit Ig domains covalently bind to the same or largely overlapping site on most Nav channel α -subunits [26,27]. Oddly however, the putative β 2- and β 4- subunit binding-site in Nav1.5 again shows important sequence differences from that on other Nav channels. Most notably, the residue equivalent to Cys895 of Nav1.7 is changed to leucine in Nav1.5 (Leu869) (Figure 4D–F). Since there are no other accessible free cysteines on the Nav1.5 extracellular surface, it will be impossible for either the β 2- or the β 4-subunit Ig domains to covalently bind Nav1.5 as they do to Nav1.7. Furthermore, the amino acid residues clustered around Nav1.7 Cys895 and which, in Nav1.7 provide additional contacts with the β 2 Ig domain, are substantially different in Nav1.5 (Figure 4F).

Taken together, this evidence suggests that the Ig domains of all four β -subunits will be unable to bind to Nav1.5 directly, although the β -subunit transmembrane and intracellular regions may still do so. As a result, the Ig domains will be free to explore a greatly extended volume space above and around the Nav1.5 channel than β -subunits attached to most other Nav channels. What then are the likely functional consequences of this difference?

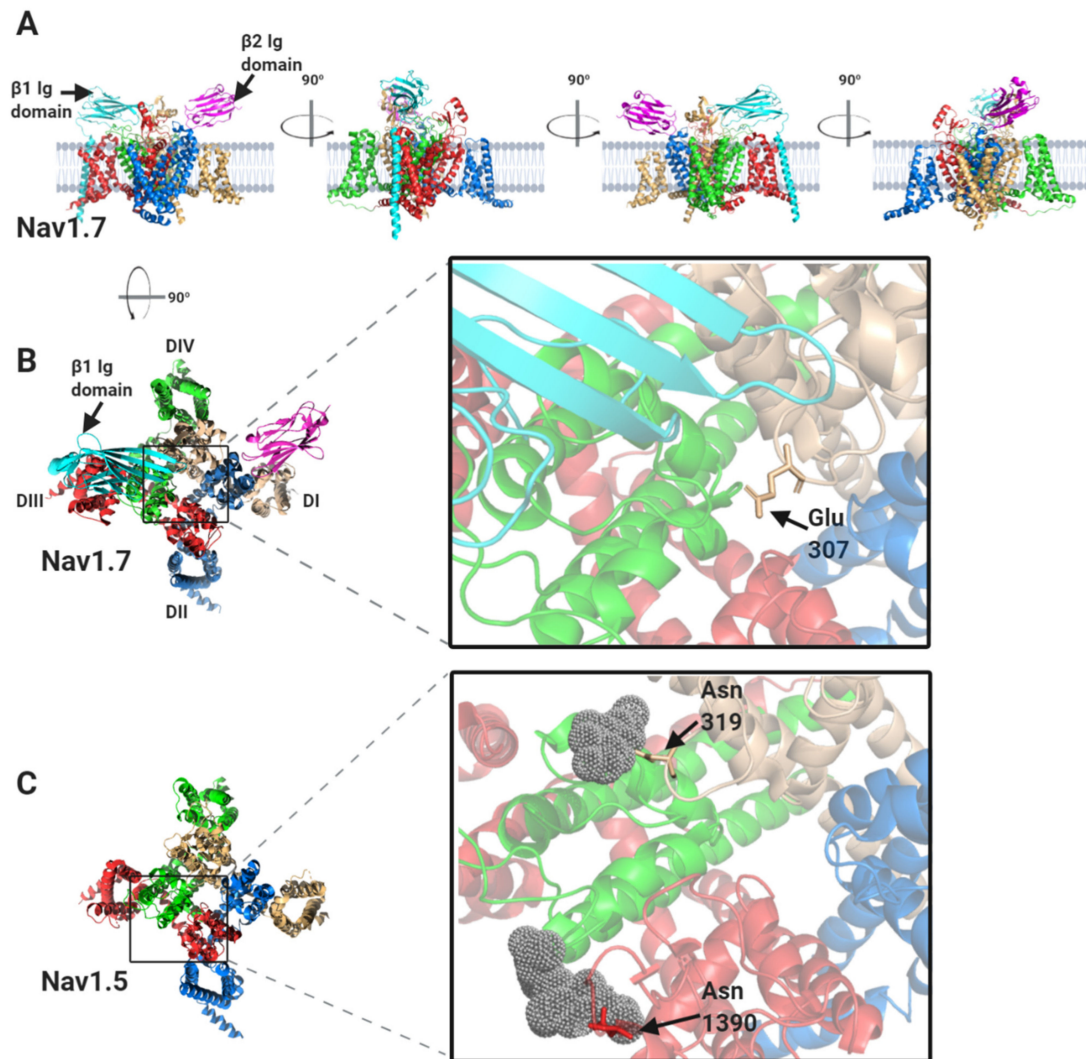


Figure 4. Cont.

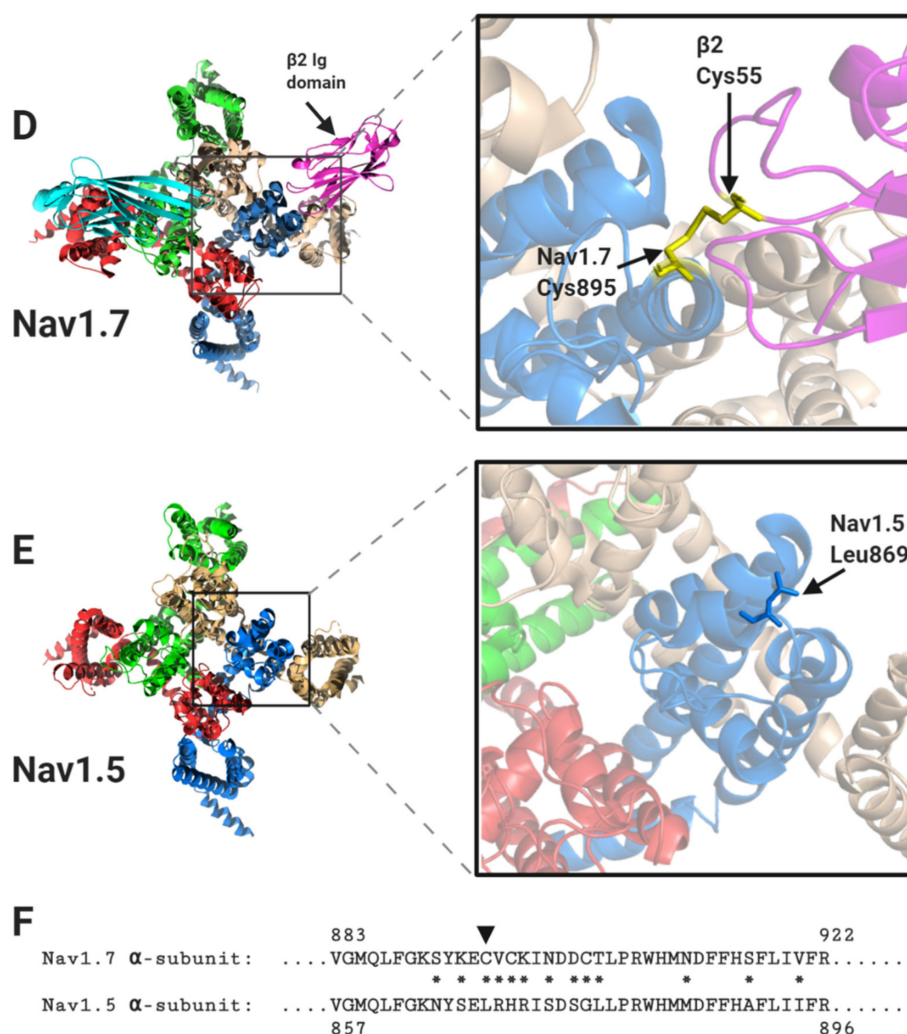


Figure 4. The binding sites for $\beta 1$ and $\beta 2$ on the Nav1.7 α -subunit and its comparison with Nav1.5. (A) Side views, each with 90° rotation, of the Nav1.7 α -subunit, with associated $\beta 1$ and $\beta 2$ -subunits. (B) Top view of the Nav1.7 α -subunit, with the $\beta 1$ Ig domain binding site on the DI, DIII and DIV extracellular loops highlighted. (C) Top view of the equivalent region of Nav1.5 α -subunit. Resolved electron density corresponding to the N-linked sugar residues mentioned in the text are shown in grey dots. (D) Top view of the Nav1.7 α -subunit with the $\beta 2$ Ig domain binding-site on DII extracellular loop highlighted. (E) Top view of the equivalent region of the Nav1.5 α -subunit. (F) Sequence alignment of human Nav1.7 and Nav1.5 α -subunits around the DII $\beta 2$ binding-site. Amino acid differences between the two sequences are indicated by asterisks. The position of the Cys895 residue in Nav1.7, noted in the text, is indicated with an arrowhead.

2. The Nav Channel β -Subunits as Cell-Adhesion Molecules

Phylogenetic analysis indicates that all four of the β -subunits are closely related to the myelin P0 family of cell-adhesion molecules (CAMs). Indeed, the $\beta 2$ and $\beta 4$ -subunit sequences are more closely related to other myelin P0-like proteins, MPZL1-3, than they are to either $\beta 1$ - or $\beta 3$ -subunits [28–30] (Figure 3C). The $\beta 1$ -subunit can bind in *trans* both to itself and to other CAMs such as neurofascins and contactins [31]. The $\beta 2$ -subunit can bind in *trans* to extracellular laminin [32]. The $\beta 3$ -subunit can bind homophilically in *cis* [20,33] and heterophilically in *trans* with neurofascins [34]. The $\beta 4$ -subunits can bind homophilically both in *cis* and *trans* [35]. In all cases, these interactions occur via the Ig domains [36]. Hence, the Nav β -subunits can be considered CAMs in their own right; albeit with the additional property of Nav channel modulation.

2.1. The Nav1.5-Associated β 1-Subunit as a CAM at the Intercalated Disc: Its Role in Ephaptic Conduction

The intercalated disc is formed from the juxtaposition of the sarcolemma membranes from adjacent cardiomyocytes and enables the cells to be mechanically and electrically coupled together [37]. It has a complex inter-digitated 'plicate' structure that ensures the inter-cellular connections are both close and continuous. Within the intercalated disc, there are distinct and structurally diverse domains each with their own specialised functions. For example, tight physical coupling at the desmosome and adherens junction help to transmit mechanical force between adjacent cells (Figure 1) [38,39]. Interspersed between these structures lie the gap junction plaques [40]. These domains contain a high local density of the protein connexin. Ventricular cardiomyocytes mostly express the connexin-43 isoform, although other isoforms are also present [41]. Connexins co-assemble on each membrane to form a symmetrical hexameric pore-containing hemichannel. Two hemichannels - one from each apposing membrane - associate in *trans* to form the functional gap junction and bind the two membranes together, so that they are no more than 2–4 nm apart, a distance that provides a tight inter-membrane seal [42]. Furthermore, a typical plaque contains several hundred closely packed gap junctions, ensuring the almost complete exclusion of other proteins from this region [41]. The central connexin pore is large enough to permit the passage of ions and small molecules [43]. Hence, the common view that electrical coupling between cardiomyocytes occurs predominantly by an electrotonic spreading mechanism in which charged ions flow passively from the cytoplasm of the 'upstream', depolarised cell to the cytoplasm of its neighbouring, 'downstream' quiescent cell via their shared gap junctions (Figure 5A) [44–46].

Surrounding and abutting the gap junction plaques lies the perinexus [47,48]. Unlike the gap junction, the perinexal membranes from adjacent cells do not interact directly, but enclose a restricted, inter-perinexal space, about 20 nm wide and extending away from the gap junction plaques for about 200 nm [48]. The perinexal membranes display a distinctive molecular composition. In particular, they contain a high local density of Nav1.5 channels that form multi-molecular two-dimensional clusters on the membrane surfaces [49]. This clustering may partly reflect an inherent tendency of Nav1.5 channels to self-associate [20]. But Nav1.5 channels are additionally stabilised by interactions with connexin-43 hemi-channels and with multi-modular cytosolic scaffolding proteins such as ankyrin-G, ZO-1 and 14-3-3 [50–52]. These interactions not only ensure the accumulation of Nav1.5, but they can also modify Nav1.5 activity. For example, ankyrin-G acts as a coordinating signalling hub, functionally connecting Nav1.5 gating with upstream kinase and phosphatase enzymes and down-stream cytoskeletal proteins [53]. In addition, 14-3-3 promotes co-operative gating behaviour between Nav1.5 α -subunits [54].

The clustering of Nav1.5 channels on the perinexal membranes, with the potential for synchronous depolarisation, ensure that activated channels on one membrane can withdraw enough sodium ions from the restricted inter-perinexal space, so that the reduced density of positive charge depolarises Nav channels on the perinexal membrane from the adjacent cell. This is the concept of ephaptic conduction, in which electrical communication between cardiomyocytes is achieved without the direct movement of sodium ions from one cell to the other (Figure 5B) [46,47,55–58]. Interestingly, perinexal Nav1.5 channels co-localise with the inwardly rectifying potassium channel Kir2.1 [59,60]. There is structural evidence that the C-terminal domains of Nav1.5 and Kir2.1 co-assemble on the cytoskeletal protein SAP97, and thereby form a functionally linked, macromolecular complex [61,62]. The Kir2.1 channel exhibits a relatively high potassium conductance when the cardiomyocyte is at the resting potential. Initially therefore, the movement of potassium ions into the perinexal space will buffer the local change in electrical potential when the Nav1.5 channels first begin to open. However, its inwardly rectifying property leads to a reduced conductance during the action potential plateau phase [63]. At this point, the entry of positively charged potassium ions into the perinexal space is minimised, just as the Nav1.5 channels are maximally depolarising and removing positively charged sodium ions. Hence, the Kir2.1 channel may act synergistically with Nav1.5 to finely regulate the rate and extent of ephaptic conduction [59].

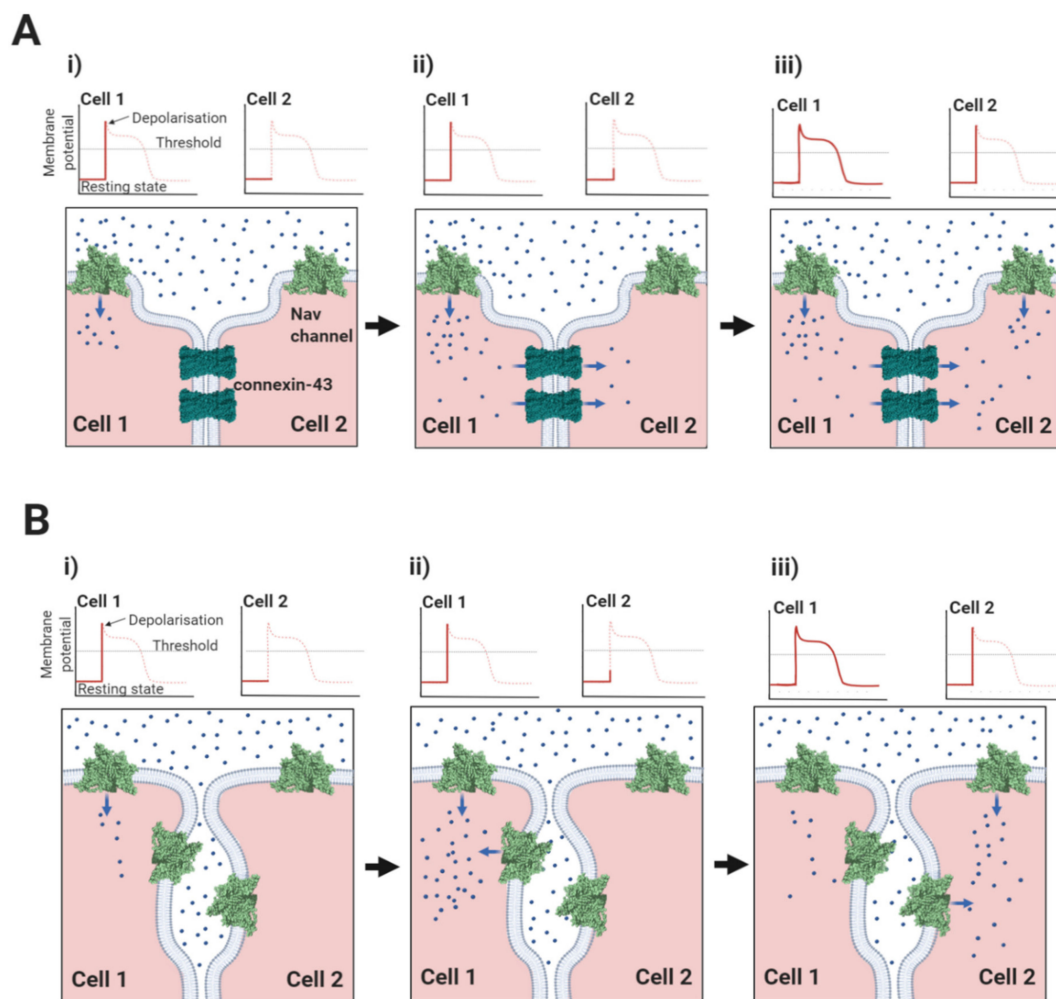


Figure 5. Comparison of electrotonic and ephaptic conduction mechanisms. **(Ai)**; In electrotonic conduction, depolarisation of cell 1 by an action potential generates a membrane potential across the gap junction comprising connexin molecules. **(Aii)**; The resulting current flow from active cell 1 to quiescent cell 2 causes its membrane to depolarise. **(Aiii)**; When this changing membrane potential rises above the threshold for Nav channel opening, an action potential is initiated in cell 2 and the excitation wave is propagated. Note, the involvement of direct charge transfer between successive cells in this process, which involves an *ohmic* transfer of charge. **(Bi)**; In ephaptic conduction, Nav channel excitation depolarises cell 1. **(Bii)**; As a result, Nav channels in the perinexal membrane of cell 1 become depolarised and there is a removal of sodium ions (and hence a net removal of positive charge) from the ephaptic space separating cells 1 and 2. **(Biii)**; The negative change in electrostatic potential within the restricted ephaptic space is enough to depolarise the transmembrane potential in cell 2, causing the activation of its Nav channels and propagation of the excitation wave. Note the absence of direct charge transfer between successive cells in this process, which involves an *electrostatic* transfer of charge. For clarity, only connexin-43 gap junction channels and Nav channels are shown, and in the action potential profiles, the Nav channel threshold has been displaced upwards.

Triggering ephaptic conduction would constitute a distinct non-canonical function of Nav channels in promoting cell-to-cell excitation, as opposed to the more familiar action potential conduction within the same cell. It could complement, or in some pathological circumstances, potentially replace electrotonic conduction mediated by gap-junctions [55,58]. Conversely, their disruption following pathological inflammatory or fibrotic change might compromise cell-cell conduction [64]. This could be in addition to disruptions in connexin-mediated cell-cell coupling [65]. It is in this context, that we suggest the unique structural features of Nav1.5 and its associated β -subunits should best be interpreted.

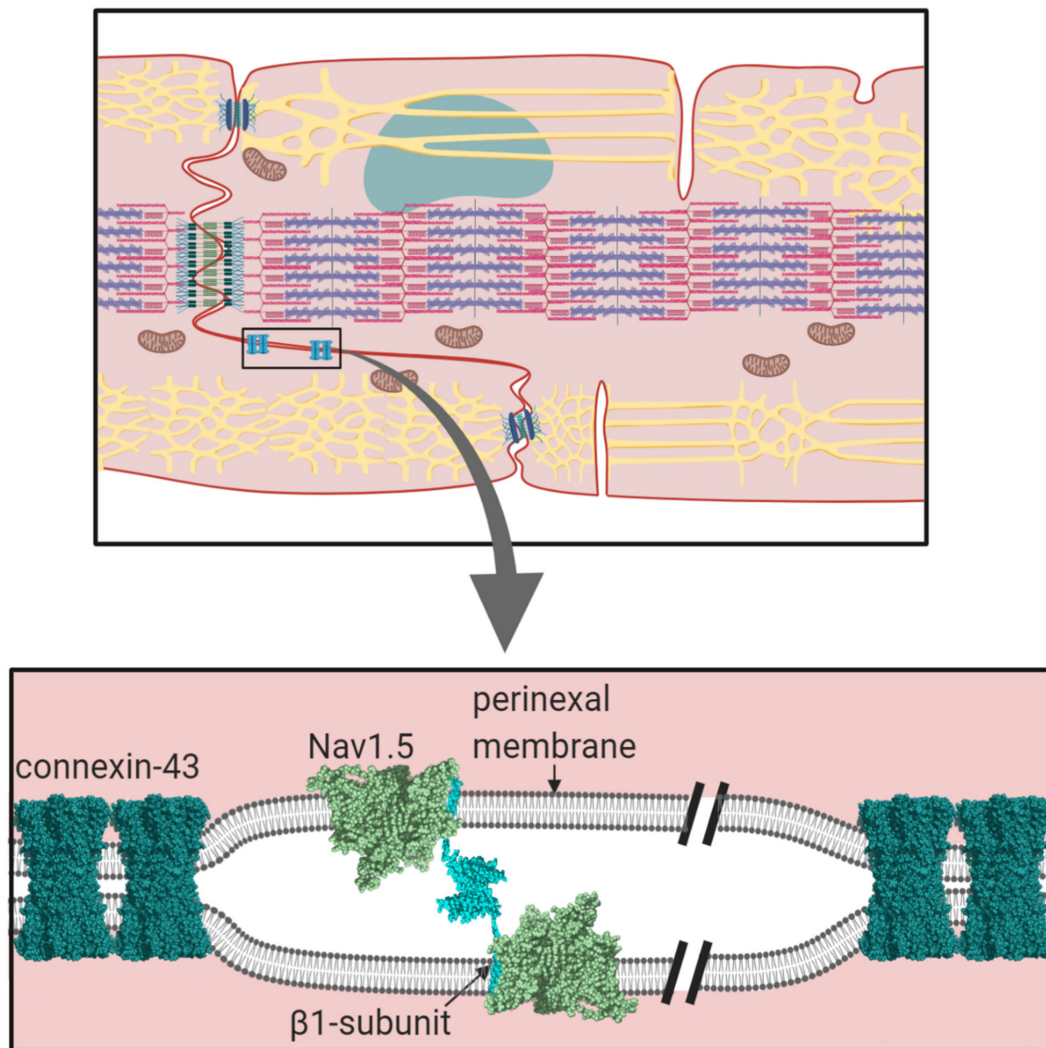


Figure 6. The proposed role for the $\beta 1$ -subunits in stabilising Nav1.5 channels on both apposing perinexal membranes, whilst also maintaining the necessary width between perinexal membranes to ensure efficient ephaptic conduction.

The perinexal Nav1.5 channels are associated with the $\beta 1$ -subunit. Recently, *Veeraraghavan, et al.*, have shown that the perinexal membranes are associated with each other by *trans* homophilic binding between apposing $\beta 1$ Ig domains [66]. However, if the $\beta 1$ Ig domain is attached to Nav1.5 in the way that it is to Nav1.7, then it would only protrude about 4–5 nm above the membrane surface (Figure 4A). In that case, the Ig domains would not be able to cover the required 20 nm distance between perinexal membranes [47]. If on the other hand, the $\beta 1$ Ig domain is not anchored onto the Nav1.5 α -subunit, then the two $\beta 1$ -subunits from apposing membranes are freer to extend their flexible necks and bridge this gap, forming *trans* cell-adhesion contacts (Figure 6). We suggest that the unique sequence differences in the DI and DIV extracellular loop domains of the Nav1.5 α -subunit compared to other Nav channels (Section 1.2, above) are specific adaptations that prevent Nav1.5 binding to the $\beta 1$ Ig domain and so facilitate this specialised cell-adhesion behaviour of the $\beta 1$ -subunit. In consequence, the *trans*-mediated $\beta 1$ Ig domain interactions help define the dimensions of the perinexal space by constraining its width to no more than about 20 nm. Mathematical modelling indicates that a gap of this order is optimum for ephaptic conduction [56].

The two interacting $\beta 1$ Ig domains form an extended antiparallel contact surface running between residues 66 and 86 (Figure 7A,B) [66,67]. In ventricular cardiomyocytes, a peptide mimetic of this binding site competitively inhibited *trans* binding between the two $\beta 1$ Ig-domain. This induced

a widening of the perinexal space, with a concomitant reduction in perinexal sodium current that precipitated arrhythmogenesis [66]. The clinical relevance of this work is supported by studies on patients with atrial fibrillation that show a correlation between arrhythmic severity and excessive widening of the atrial perinexal membranes [68]. Moreover, there are two independent *SCN1b* mutations within or close to this region that are associated with Brugada syndrome: a charge-neutralising Arg to His change at residue 85 and a charge-neutralising Glu to Gln mutation at residue 87 (Figure 7B) [69,70]. Taken together, these multiple structural, anatomical, pathological and experimental data sets not only support a role for ephaptic conduction between cardiomyocytes, but also implicate the structure, geometry and *trans*-binding behaviour of the β 1-subunit as specific adaptations that are critical for this mechanism.

When the cardiomyocytes are at rest, the inter-perinexal space is largely enclosed, such that it is minimally influenced by its surrounding extracellular fluid. This too should increase the ability of activated Nav1.5 channels to remove enough positive charge to induce ephaptic conduction. Nevertheless, there must be some way for the electrolyte composition of the perinexal space to be reset between excitation events. This could be facilitated by geometrical changes produced by the cardiomyocyte contractions if they transiently enhance the accessibility of the perinexal space to the extracellular milieu. Real-time *in vivo* imaging of ventricular cardiomyocytes has identified surprisingly large flexing movements in the perinexus during the propagation of cell-to-cell contraction [71]. A consequence of these cellular and membrane movements will be the rhythmic stretching and relaxing of the *trans*-associated β 1-subunits. Here, the disordered and spring-like neck region of the β 1-subunit, connecting its rigid Ig domain to its rigid transmembrane alpha-helix might enable some strain-absorbing movement of the β 1-subunit. However, as noted above, the β 1 peptide mimetic can not only gain access to the perinexal space, it can also disrupt the *trans*-binding between β 1 Ig domains [66]. This implies that the *trans* binding must—at least to some degree—be dynamic, perhaps reflecting a periodic dissociation and rebinding during the stretching cycle.

The β 1-subunit can bind to cytosolic ankyrin-G and ankyrin-B via its intracellular region. But this interaction is abolished if a critical intracellular tyrosine residue, Y181, is phosphorylated by Fyn kinase [72,73]. In cardiomyocytes, the tyrosine-phosphorylated form of β 1 is present only at the intercalated disc, where it interacts with Nav1.5 and the CAM cadherin, but does not bind ankyrin-G. The non-phosphorylated β 1-subunit is present on the lateral membranes [74]. Of course, there could be many functional reasons for this pattern. For example, phosphorylation may be a targeting signal to direct β 1-subunits to the intercalated disc [15]. Alternatively, the β 1-subunit may be actively phosphorylated at the intercalated disc in response to changes in membrane stretching or other physiological signals. This would change the proportion of β 1 that could connect to the cytoskeleton via ankyrin-G and thus modify cell-adhesion, perhaps even during a contraction cycle. One may speculate that the β 1-mediated *trans* contacts could be further modulated via the alternatively spliced β 1B isoform (Figure 3A) [15]. Since this isoform is secreted, it could in theory interrupt and fine-tune the *trans*-binding, if present in the perinexal space. There is as yet no direct evidence for this proposal, but a mutation in the β 1B isoform is linked to Brugada syndrome [75].

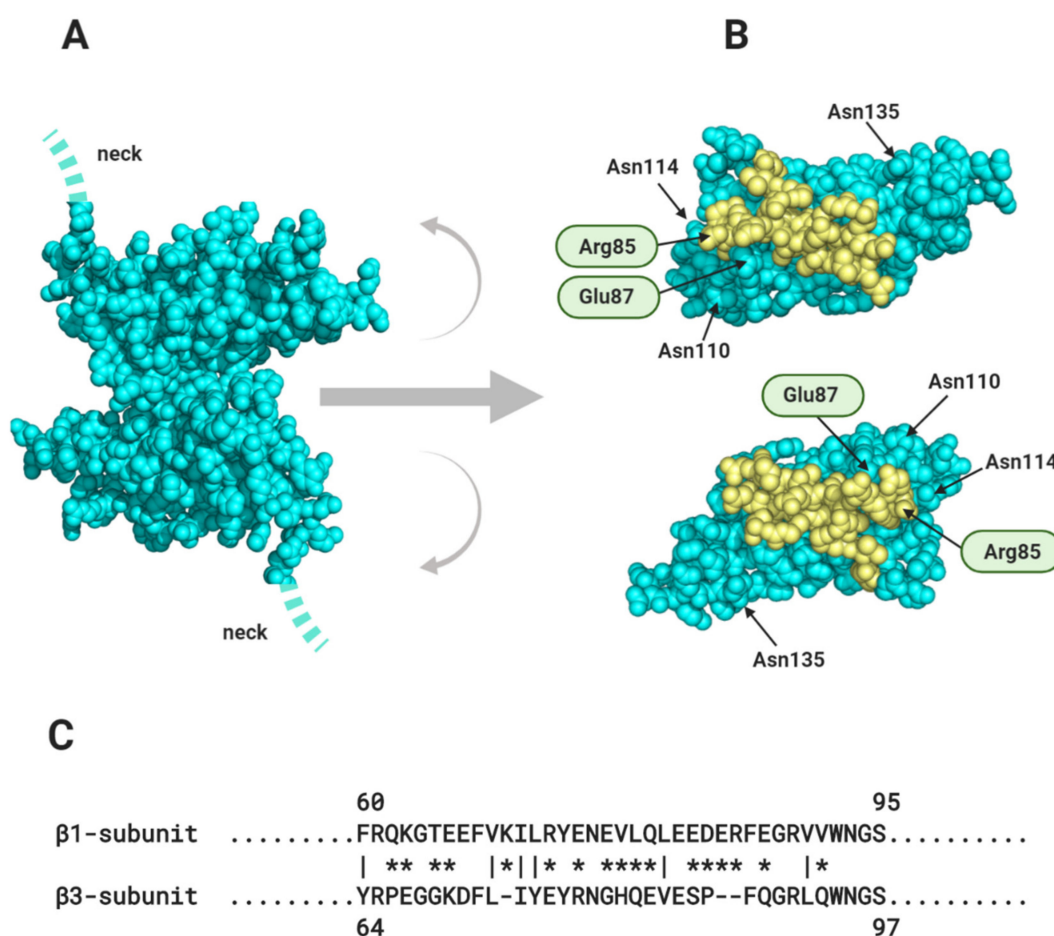


Figure 7. The proposed contact surface between the trans-interacting β 1 Ig domains. (A) The antiparallel arrangement of β 1 Ig domains. (B) the two β 1 Ig domains ‘peeled back’ to reveal the contact surface proposed by [66]. The location of two Brugada mutations (Arg85 and Glu87), mentioned in the text are indicated. Potential N-linked glycosylation sites, Asn110, Asn114 and Asn135 are indicated. (C) Sequence alignment between β 1 and β 3 Ig domains within the proposed contact surface, showing low sequence identity. Non-conservative changes are shown with asterisks and conservative changes with vertical lines.

2.2. Do Other Nav Channel β -Subunits Facilitate Ephaptic Conduction?

Although the β 3 and β 1-subunits show the closest overall sequence similarity (Figure 3C), there are localised sequence differences between them that could suggest functional specialisation. In particular, the sequence of the β 1 Ig domain *trans* cell-adhesion binding site is not conserved in β 3 (Figure 7C) [76] and the evidence that β 3 can act as a homophilic *trans* CAM is mixed [76,77]. We therefore suggest that unlike β 1, the β 3-subunit may not play a major role in stabilising the perinexal space by *trans*-mediated cell-adhesion. On the other hand, when expressed alone in HEK293 cells, the β 3-subunits bind homophilically in *cis*, using their Ig domains [19,20,33]. Super-resolution imaging experiments show that when co-expressed with Nav1.5, the β 3-subunit affects the relative geometry between Nav1.5 channel α -subunits, possibly by promoting particular orientations of individual Nav1.5 α -subunit dimers within larger clusters [20]. This is consistent with a *cis*-mediated β 3-subunit effect. The *cis*-interacting β 3-subunit Ig domains could cross-link Nav1.5 channels within each perinexal membrane and thus contribute lateral stability to the channel clusters whilst the β 1-subunit provides structural stability between apposing perinexal membranes.

Binding of the $\beta 2$ -subunit to Nav1.5 cannot be detected by immunoprecipitation, when tested in transfected HEK-cells [14]. Yet the $\beta 2$ -subunit can be immunoprecipitated together with Nav1.5 from heart tissue [78] and mutations in the $\beta 2$ cytosolic region compromise the trafficking efficiency of Nav1.5 in cardiomyocytes [2]. Hence, additional cardiomyocyte-specific protein contacts are likely to be required to stabilise $\beta 2$ -binding to Nav1.5 in its normal physiological context. Interestingly, the Ig domains of the $\beta 1$ and $\beta 2$ -subunits can interact in *trans*, but the association requires the presence of a sequence within the $\beta 2$ -subunit cytoplasmic region that contains a putative casein kinase II phosphorylation site [31]. This raises the possibility that *trans* heterophilic interactions between $\beta 1$ and $\beta 2$ Ig domains may occur across the perinexal space, yet be regulated by signal transduction events acting on the cytosolic face of the membranes [2].

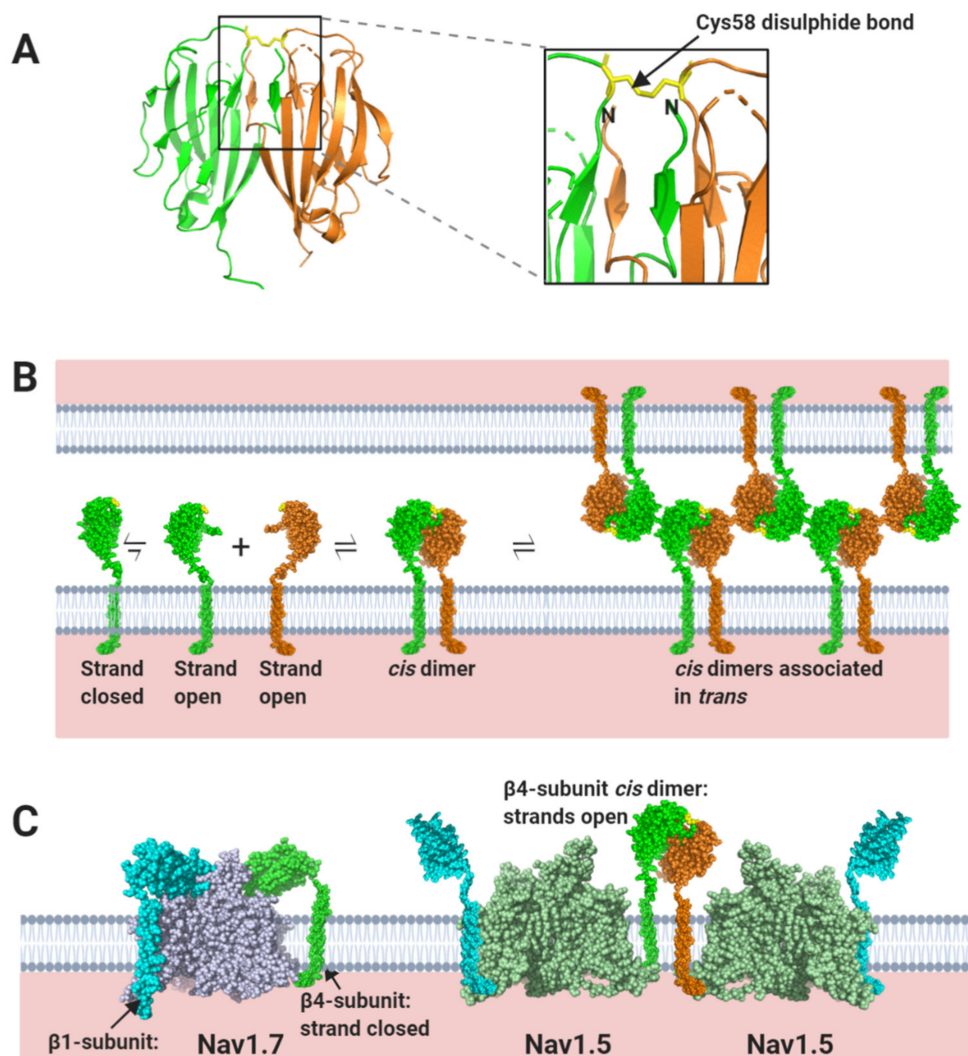


Figure 8. The $\beta 4$ -subunit Ig domain can associate in both *cis* and *trans*. (A) The disulphide-bonded, *cis*-interacting, dimeric $\beta 4$ -subunit Ig domain (PDB: 5XAW) with the Cys58 disulphide and the strand swap N-terminal regions highlighted. (B) Proposed model for *trans*-interacting, $\beta 4$ -subunit Ig domain *cis*-dimers, based on the model discussed in the text [79]. (C) Proposed association of the $\beta 4$ - and $\beta 1$ -subunits on Nav1.7 and Nav1.5 α -subunits. Note, to clarify the structural details in (A) and the cartoon models in (B) and (C), the two identical $\beta 4$ Ig domains and $\beta 4$ -subunits are coloured differently, in green and orange.

The homophilic cell-adhesion contacts of the $\beta 4$ Ig domain have been studied using crystallographic analysis, site-specific cross-linking with unnatural amino acids and cell-adhesion assays. The $\beta 4$ Ig

domain can be isolated as a dimer, stabilised by two striking features. Firstly, the presence of an inter-subunit disulphide bond between the Cys58 residue on each Ig domain. Secondly, a reciprocal strand-swap interaction, in which the first seven N-terminal amino-acid residues from one Ig domain interact with residues on the partner Ig domain (Figure 8A) [79]. N-terminal strand-swapping is a known feature of several *trans*-mediated CAMs that contain Ig domains, including cadherins in the adherens junctions and desmogleins in the desmosomes [80–82]. In the case of $\beta 4$ however, the strand-swapped, disulphide-bonded Ig domain dimer is proposed to assemble on the same membrane in a *cis*-interaction. In this process, the N-terminal residues that undergo swapping must first undock from their binding site within the ‘closed’ monomer, to generate an ‘open’ monomer, which is then capable of *cis*-dimerisation (Figure 8B). A $\beta 4$ Ig domain in which the Cys58 residue was changed to alanine, crystallised as a monomer in the asymmetric unit and the N-terminal strand was not resolved [26], suggesting that this conformation might correspond to the monomeric ‘open’ state. It has been further proposed that at the cell-surface, the $\beta 4$ *cis* dimers, then interact in *trans* to promote cell-adhesion (Figure 8B) [35,79]. It is interesting to note that neither the $\beta 1$ -subunit, nor the $\beta 3$ -subunit Ig domains can form similar strand-swap dimers, because their N-terminal strands are covalently locked in place via an intramolecular disulphide bond [12,33,76] (Figure 3B).

These structural insights have an important implication. If $\beta 4$ is paired with most Nav channel α -subunits, its Cys58 residue will form a disulphide bond with the free cysteine on the α -subunit DII S5-P extracellular loop site [25] (e.g., Nav1.7; Figures 4D and 8C). But this would inhibit formation of the Cys58-mediated $\beta 4$ *cis* dimer (Figure 8A,B). On the other hand, the Nav1.5 α -subunit lacks a free DII, S5-P cysteine. So, it is not possible for Nav1.5 to covalently bind the $\beta 4$ -subunit Ig domain (Section 1.2.). Nevertheless, the interaction between the $\beta 4$ -subunit and Nav1.5 is stable enough to be detected by immunoprecipitation when co-expressed in HEK293 cells [83]. Presumably, $\beta 4$ must still bind to Nav1.5 via other sites such as the transmembrane alpha-helix and/or the cytoplasmic region. This will leave any Nav1.5-associated, $\beta 4$ -subunit Ig domains free to form disulphide-bonded, homophilic dimers (Figure 8C). Thus, potentially, the $\beta 4$ -subunit could facilitate not only *cis*- but also *trans*-mediated Nav1.5 cross-linking (Figure 8B,C). The overall dimensions of the $\beta 4$ subunit are similar to $\beta 1$ [17]. The $\beta 4$ and $\beta 2$ -subunits can be detected very close to - but distinct from - the intercalated disc gap junctions [5], suggesting a likely perinexal location. It is tempting to speculate that the $\beta 4$ (and probably $\beta 2$) subunits could help stabilise both the width of the perinexal space and the clustering of Nav1.5 within this region by facilitating extensive *cis* and *trans*-mediated associations.

2.3. Nav Channels and β -Subunits on the Lateral Membrane: A Role in Mechanosensing?

A major fraction of the Nav1.5 channels on the lateral membrane are sequestered into lipid rafts and caveolae [84,85]. The caveolae are cholesterol-rich microdomains stabilised by the intrinsic scaffold membrane protein caveolin and the peripheral, cytosolic protein cavin [86]. Palmitoylation is commonly thought to act as a targeting signal that directs proteins into these structures [87]. Interestingly, the transmembrane alpha-helix of the $\beta 1$ and $\beta 3$ -subunits (but not the $\beta 2$ and $\beta 4$ -subunits) contains a juxtamembrane cysteine residue, located at the cytoplasmic interface that fits the consensus for a palmitoylation site [16,17]. Recent work confirms that $\beta 1$ is indeed palmitoylated at this residue (Cys162). However, mutational abolition of the Cys162 residue does not prevent $\beta 1$ targeting to detergent-resistant membrane fractions (assumed to correspond to lipid rafts), although it does reduce the steady-state level of the $\beta 1$ -subunit at the plasma membrane [88]. Within the caveolae, the Nav1.5 and β -subunit complexes are co-clustered with both Kir2.1 and the Kv4.2/4.3 channels responsible for the transient outward potassium current [84,89,90]. Surprisingly, the Nav channel $\beta 1$ -subunit binds to and regulates the Kv4.2/4.3 channels [91]. This opens the potential for mutual control of both channels via Nav $\beta 1$ - especially so on the restricted and crowded caveolar membrane. The caveolae also sequester integrins, required for cell-adhesion to extracellular matrix proteins such as collagen and fibronectin, together with the integrin-activated signalling enzyme, Fyn kinase [86,92]. However, since the caveolae are highly invaginated, rosette-like clusters, it is not clear whether the sequestered

integrins can bind extracellular matrix proteins under these conditions; neither is it clear whether the sequestered ion channels can be active [93]. Yet there is evidence that caveolin can regulate integrin activity [94] and in turn, both integrins and caveolin can modulate Nav1.5, Kir2.1 and Kv4.2/4.3 channels [95–97].

A possible explanation for these observations is that caveolae act as sensors for mechanical stress and respond dynamically to changes in cell deformation [98]. In particular, the cell stretching initiates a rapid dissociation of the cavin coat and a ‘flattening’ of the caveolae membrane. This mechanism increases the surface area of the plasma membrane and helps buffer against stretching forces [99,100]. A further consequence is that the integrins, ion channels and signal transduction enzymes are repartitioned into the plasma membrane, but probably remain as a macromolecular complex. This translocation is followed by an increased integrin-stimulated ERK signalling, which is caveolin-dependent [93]. Since ERK is a down-stream target of activated Fyn kinase [101], this suggests that the translocation of the integrin/ion channel complex into the wider plasma membrane can enhance integrin-dependent Fyn-kinase activation, perhaps by enabling greater access of the integrins to their extracellular matrix ligands. Activated Fyn kinase also phosphorylates Nav1.5, inducing a depolarising shift in the $V_{1/2}$ of steady-state inactivation, thus increasing the fraction of functionally active Nav1.5 channels on the membrane [102]. Furthermore, Nav1.5 is a mechanosensor and the membrane flexing itself will affect channel gating. In particular, the Nav1.5 channel responds to physiological levels of mechanical membrane stress with a hyperpolarising shift to the $V_{1/2}$ of steady-state inactivation [103,104]. Remarkably, the β 1-subunit further amplifies this hyperpolarising shift [105]. The combination of increased Nav1.5 excitability via integrin-activated Fyn-kinase signalling, with the opposite mechanosensitive response of Nav1.5 and its β 1-subunit may act to finely balance the need to integrate different cell-adhesion signals, whilst also protecting against excessive mechanical stress over a large voltage range. The β 3-subunit enhances the mechano-induced acceleration of both activation and inactivation kinetics, but unlike β 1, it does not affect the mechanosensitive shifts in steady-state parameters [105]. The structural explanation for these differences between β 1 and β 3-subunits and indeed their functional significance, is not clear.

The β -subunits exposed on the lateral membrane can interact with extracellular matrix proteins. For example, the β 2-subunit can bind in *trans* to laminin, a known component of the heart extracellular matrix [32]. But there is relatively little β 2-subunit exposed on the cardiomyocyte lateral membrane [5]. Another possibility is that β 1-subunits exposed on the surface of the lateral membrane may interact homophilically with β 1-subunits and other CAMs on adjacent cell types [31,34]. For example, during cardiac fibrosis, there is an enhanced proliferation of myofibroblasts that express several different Nav channels including Nav1.5, together with the β 1-subunit [106]. Myofibroblasts can form aberrant electrical connections to the cardiomyocytes, which likely adds additional and potentially pro-arrhythmic membrane capacitance [107]. Whether the contacts between cardiomyocytes and myofibroblasts involve *trans*-cell adhesion contacts between β 1-subunits remains to be determined.

2.4. Nav β -Subunits and Neuronal Channels in the T-Tubules

The neuronal Nav channels localised within the T-tubules are predominantly associated with the β 1 and β 3-subunits [5]. These Nav α -subunits all lack a glycosylation site in their DI, S5-P extracellular loop, equivalent to Asn319 in Nav1.5 [9]. Hence, it is likely that the β 1 and β 3 Ig domains will bind onto these Nav α -subunits in a manner more like Nav1.7 than Nav1.5 (Figure 4A,B). As the T-tubule width is significantly greater than 20 nm (and is often more than 100 nm) [108], any direct *trans*-mediated binding of β 1 Ig domains between opposite membrane faces of the T-tubules is unlikely. There is evidence that CAMs such as laminin can enter the lumen of large-diameter T-tubules [109]. So, cell-adhesion-type functions for T-tubular β -subunits cannot be ruled out. In mice, deletion of the *SCN1b* gene perturbs the interaction between T-tubular Nav channels and NCX complexes, with a consequent dysregulation of calcium homeostasis, suggesting a structural role to facilitate excitation-contraction coupling [110].

3. Conclusions and Unsolved Problems

On the cardiomyocyte membranes, the Nav channels form heterogeneous, multi-component macromolecular clusters, rather than remain as isolated molecules [111]. There is no necessary requirement for every Nav α -subunit to have an identical stoichiometry with any associated β -subunit [17]. Examples from other ion-channels show that the behaviour of membrane-bound clusters can change depending on variations in subunit ratios [112]. In such assemblies, individual protein components can have more than one function, depending on the physiological context. Although originally identified by their direct effects on channel gating, it is now clear that the Nav β -subunits extend their functions to include cell-adhesion and mechano-sensing and in doing so, raise further questions:

3.1. Evolutionary Relationship between Nav β -Subunits and Other CAMs

The Ig domain superfamily has deep evolutionary roots that pre-date the divergence of vertebrate and invertebrate lineages [113]. Yet the Nav channel β -subunits have only been discovered in vertebrate genomes, where they cluster together with members of the Ig domain-containing CAM family [30]. This close evolutionary relationship raises the intriguing possibility that homologues such as the MPZL1-3 group of proteins (Figure 3C), might act as additional Nav channel modulators. At least some of these proteins are expressed in heart tissue [114].

Although lacking β -subunits, invertebrate Nav channels do possess associated proteins that modulate gating and trafficking behaviour of their Nav channels. The best characterised are members of the TipE family [115]. However, these proteins show no sequence or structural similarity to vertebrate β -subunits and must have independently evolved their Nav channel-modulating behaviour. It will be interesting to see whether the TipE proteins can act as CAMs, or whether cell-adhesion is a unique feature of the vertebrate β -subunits.

3.2. The Biophysics of Nav β -Subunit Cell-Adhesion

We currently lack a quantitative understanding of the *trans*-mediated binding events facilitated by the β -subunits. For example, it would be interesting to know if the contacts between individual β 1 Ig domains at the perinexus are strong and stable or individually weak enough to dissociate and rebind rapidly. The latter case might be more likely given the dynamic nature of membrane movements at the intercalated disc during the contraction, relaxation cycle [71]. The application of new biophysical techniques such as atomic force microscopy and traction force microscopy [116], combined with more traditional biochemical and molecular genetic techniques will be needed to address these questions.

3.3. The Role of N-Linked Glycosylation

Membrane proteins are generally N-linked glycosylated, with complex, branching sugar residues, often tipped with sialic acid moieties [117]. The role of N-linked glycosylation in the trafficking of Nav channels, including Nav1.5 - is well-established [118]. There is also evidence that the negatively charged sialic acids on N-linked glycans of Nav channel α and β -subunits can modulate channel gating [119]. In addition, the relatively large and bulky N-linked glycans can potentially modulate the strength and even the possibility of protein-protein interactions occurring. A good example is described above for the case of the β 1 Ig domain binding to Nav1.5, and the likely role of the glycosylated Asn319 residue in preventing binding of the β 1 Ig domain (Section 1.2, Figure 4C). Another example is in the model proposed for β 1- *trans* cell-adhesion. Here, the putative *trans*-binding motif on the β 1 Ig domain surface is surrounded by four of its five potential N-linked glycosylation sites (Section 2.1, Figure 7B). Could the strength of this interaction be fine-tuned by for example, developmentally regulated changes in the nature and extent of N-linked glycosylation?

3.4. Ephaptic Conduction in the Heart and Elsewhere

In cardiomyocytes, ephaptic conduction occurs in close association with gap junction structures mediating electrotonic conduction (Section 2.1, Figure 5), suggesting that both processes occur to relative extents, that might vary under different conditions [120]. It is likely that there are other biological situations where the necessary conditions for ephaptic conduction apply. Potential examples include the repetitive firing that occur in neuroendocrine supraoptic nucleus neurones [121,122] and the escape reflex triggered by activation of the goldfish Mauthner neurone [123]. Interestingly, the R85H mutation in the $\beta 1$ Ig domain, that compromises ephaptic conduction between cardiomyocytes [66] (Section 2.1, Figure 7B), also predisposes to epilepsy [124], perhaps hinting at a similar role in neurones.

3.5. Clinical Implications

Assuming that electrical signalling between cardiomyocytes occurs both by electrotonic and ephaptic mechanisms, then a drug that inhibits the *trans*-mediated cell-adhesion between perinexal $\beta 1$ -subunits might reduce the signal propagation through cardiac muscle, whilst not completely preventing it. This could potentially reduce triggering of post-infarct arrhythmias [125]. Conversely, drugs that stabilise these interactions could be useful as a treatment for other forms of arrhythmias such as Brugada syndrome in which re-entrant arrhythmia results from a conduction slowing substrate [66]. It might also be possible to target specific β -subunit signalling pathways, for example the phosphorylation of the $\beta 1$ -subunit cytoplasmic region [126]. These are quite speculative, yet potentially attractive hypotheses that require further investigations. More broadly, the increasing emphasis on the cell-adhesion roles of Nav β -subunits in both healthy and pathological states, offers a more balanced perspective on these proteins and could open completely new avenues for therapy.

Author Contributions: Conceptualization, investigation and writing, S.C.S., C.L.-H.H. and A.P.J. All authors have read and agreed to the published version of the manuscript.

Funding: S.C.S was supported by British Heart Foundation project grants PG/14/79/31102 and PG/19/59/34582 (to S.C.S., C.L.-H.H., and A.P.J.) and by Isaac Newton Trust Grant G101770.

Acknowledgments: The figures were created with BioRender.com.

Conflicts of Interest: The authors declare no conflict of interest.

References

1. Sweeney, H.L.; Hammers, D.W. Muscle Contraction. *Cold Spring Harb. Perspect. Biol.* **2018**, *10*. [[CrossRef](#)] [[PubMed](#)]
2. Cortada, E.; Brugada, R.; Verges, M. Trafficking and Function of the Voltage-Gated Sodium Channel beta2 Subunit. *Biomolecules* **2019**, *9*, 604. [[CrossRef](#)] [[PubMed](#)]
3. DeMarco, K.R.; Clancy, C.E. Cardiac Na Channels: Structure to Function. *Curr. Top. Membr.* **2016**, *78*, 287–311. [[CrossRef](#)] [[PubMed](#)]
4. Veeraraghavan, R.; Gyorke, S.; Radwanski, P.B. Neuronal sodium channels: Emerging components of the nano-machinery of cardiac calcium cycling. *J. Physiol.* **2017**, *595*, 3823–3834. [[CrossRef](#)]
5. Maier, S.K.; Westenbroek, R.E.; McCormick, K.A.; Curtis, R.; Scheuer, T.; Catterall, W.A. Distinct subcellular localization of different sodium channel alpha and beta subunits in single ventricular myocytes from mouse heart. *Circulation* **2004**, *109*, 1421–1427. [[CrossRef](#)] [[PubMed](#)]
6. Fraser, J.A.; Huang, C.L.; Pedersen, T.H. Relationships between resting conductances, excitability, and t-system ionic homeostasis in skeletal muscle. *J. Gen. Physiol.* **2011**, *138*, 95–116. [[CrossRef](#)] [[PubMed](#)]
7. Pedersen, T.H.; Huang, C.L.-H.; Fraser, J.A. An analysis of the relationships between subthreshold electrical properties and excitability in skeletal muscle. *J. Gen. Physiol.* **2011**, *138*, 73–93. [[CrossRef](#)]
8. Ahern, C.A.; Payandeh, J.; Bosmans, F.; Chanda, B. The hitchhiker's guide to the voltage-gated sodium channel galaxy. *J. Gen. Physiol.* **2016**, *147*, 1–24. [[CrossRef](#)]
9. Nishino, A.; Okamura, Y. Evolutionary History of Voltage-Gated Sodium Channels. *Handb. Exp. Pharmacol.* **2018**, *246*, 3–32. [[CrossRef](#)]

10. Yan, Z.; Zhou, Q.; Wang, L.; Wu, J.; Zhao, Y.; Huang, G.; Peng, W.; Shen, H.; Lei, J.; Yan, N. Structure of the Nav1.4-beta1 Complex from Electric Eel. *Cell* **2017**, *170*, 470–482.e11. [[CrossRef](#)]
11. Pan, X.; Li, Z.; Zhou, Q.; Shen, H.; Wu, K.; Huang, X.; Chen, J.; Zhang, J.; Zhu, X.; Lei, J.; et al. Structure of the human voltage-gated sodium channel Nav1.4 in complex with beta1. *Science* **2018**, *362*. [[CrossRef](#)] [[PubMed](#)]
12. Shen, H.; Liu, D.; Wu, K.; Lei, J.; Yan, N. Structures of human Nav1.7 channel in complex with auxiliary subunits and animal toxins. *Science* **2019**, *363*, 1303–1308. [[CrossRef](#)] [[PubMed](#)]
13. Pan, X.; Li, Z.; Huang, X.; Huang, G.; Gao, S.; Shen, H.; Liu, L.; Lei, J.; Yan, N. Molecular basis for pore blockade of human Na(+) channel Nav1.2 by the mu-conotoxin KIIIA. *Science* **2019**, *363*, 1309–1313. [[CrossRef](#)] [[PubMed](#)]
14. Jiang, D.; Shi, H.; Tonggu, L.; Gamal El-Din, T.M.; Linaeus, M.J.; Zhao, Y.; Yoshioka, C.; Zheng, N.; Catterall, W.A. Structure of the Cardiac Sodium Channel. *Cell* **2020**, *180*, 122–134.e110. [[CrossRef](#)]
15. Edokobi, N.; Isom, L.L. Voltage-Gated Sodium Channel beta1/beta1B Subunits Regulate Cardiac Physiology and Pathophysiology. *Front. Physiol.* **2018**, *9*, 351. [[CrossRef](#)]
16. Brackenbury, W.J.; Isom, L.L. Na Channel beta Subunits: Overachievers of the Ion Channel Family. *Front. Pharmacol.* **2011**, *2*, 53. [[CrossRef](#)]
17. Namadurai, S.; Yereddi, N.R.; Cusdin, F.S.; Huang, C.L.; Chirgadze, D.Y.; Jackson, A.P. A new look at sodium channel beta subunits. *Open Biol.* **2015**, *5*, 140192. [[CrossRef](#)]
18. Patino, G.A.; Isom, L.L. Electrophysiology and beyond: Multiple roles of Na⁺ channel beta subunits in development and disease. *Neurosci. Lett.* **2010**, *486*, 53–59. [[CrossRef](#)]
19. Salvage, S.C.; Zhu, W.; Habib, Z.F.; Hwang, S.S.; Irons, J.R.; Huang, C.L.H.; Silva, J.R.; Jackson, A.P. Gating control of the cardiac sodium channel Nav1.5 by its beta3-subunit involves distinct roles for a transmembrane glutamic acid and the extracellular domain. *J. Biol. Chem.* **2019**. [[CrossRef](#)]
20. Salvage, S.C.; Rees, J.S.; McStea, A.; Hirsch, M.; Wang, L.; Tynan, C.J.; Reed, M.W.; Irons, J.R.; Butler, R.; Thompson, A.J.; et al. Supramolecular clustering of the cardiac sodium channel Nav1.5 in HEK293F cells, with and without the auxiliary beta3-subunit. *FASEB J.* **2020**, *34*, 3537–3553. [[CrossRef](#)]
21. Zhu, W.; Voelker, T.L.; Varga, Z.; Schubert, A.R.; Nerbonne, J.M.; Silva, J.R. Mechanisms of noncovalent beta subunit regulation of NaV channel gating. *J. Gen. Physiol.* **2017**. [[CrossRef](#)] [[PubMed](#)]
22. Hakim, P.; Gurung, I.S.; Pedersen, T.H.; Thresher, R.; Brice, N.; Lawrence, J.; Grace, A.A.; Huang, C.L. Scn3b knockout mice exhibit abnormal ventricular electrophysiological properties. *Prog. Biophys. Mol. Biol.* **2008**, *98*, 251–266. [[CrossRef](#)] [[PubMed](#)]
23. Ko, S.H.; Lenkowski, P.W.; Lee, H.C.; Mounsey, J.P.; Patel, M.K. Modulation of Na(v)1.5 by beta1- and beta3-subunit co-expression in mammalian cells. *Pflug. Arch.* **2005**, *449*, 403–412. [[CrossRef](#)] [[PubMed](#)]
24. Chen, C.; Calhoun, J.D.; Zhang, Y.; Lopez-Santiago, L.; Zhou, N.; Davis, T.H.; Salzer, J.L.; Isom, L.L. Identification of the cysteine residue responsible for disulfide linkage of Na⁺ channel alpha and beta2 subunits. *J. Biol. Chem.* **2012**, *287*, 39061–39069. [[CrossRef](#)] [[PubMed](#)]
25. Yu, F.H.; Westenbroek, R.E.; Silos-Santiago, I.; McCormick, K.A.; Lawson, D.; Ge, P.; Ferriera, H.; Lilly, J.; DiStefano, P.S.; Catterall, W.A.; et al. Sodium channel beta4, a new disulfide-linked auxiliary subunit with similarity to beta2. *J. Neurosci.* **2003**, *23*, 7577–7585. [[CrossRef](#)]
26. Gilchrist, J.; Das, S.; Van Petegem, F.; Bosmans, F. Crystallographic insights into sodium-channel modulation by the beta4 subunit. *Proc. Natl. Acad. Sci. USA* **2013**, *110*, E5016–E5024. [[CrossRef](#)]
27. Das, S.; Gilchrist, J.; Bosmans, F.; Van Petegem, F. Binary architecture of the Nav1.2-beta2 signaling complex. *eLife* **2016**, *5*. [[CrossRef](#)]
28. Molinarolo, S.; Granata, D.; Carnevale, V.; Ahern, C.A. Mining Protein Evolution for Insights into Mechanisms of Voltage-Dependent Sodium Channel Auxiliary Subunits. *Handb. Exp. Pharmacol.* **2018**, *246*, 33–49. [[CrossRef](#)]
29. Kusano, K.; Thomas, T.N.; Fujiwara, K. Phosphorylation and localization of protein-zero related (PZR) in cultured endothelial cells. *Endothelium* **2008**, *15*, 127–136. [[CrossRef](#)]
30. Chopra, S.S.; Watanabe, H.; Zhong, T.P.; Roden, D.M. Molecular cloning and analysis of zebrafish voltage-gated sodium channel beta subunit genes: Implications for the evolution of electrical signaling in vertebrates. *BMC Evol. Biol.* **2007**, *7*, 113. [[CrossRef](#)]
31. McEwen, D.P.; Isom, L.L. Heterophilic interactions of sodium channel beta1 subunits with axonal and glial cell adhesion molecules. *J. Biol. Chem.* **2004**, *279*, 52744–52752. [[CrossRef](#)] [[PubMed](#)]

32. Jansson, K.H.; Castillo, D.G.; Morris, J.W.; Boggs, M.E.; Czymmek, K.J.; Adams, E.L.; Schramm, L.P.; Sikes, R.A. Identification of beta-2 as a key cell adhesion molecule in PCa cell neurotropic behavior: A novel ex vivo and biophysical approach. *PLoS ONE* **2014**, *9*, e98408. [[CrossRef](#)] [[PubMed](#)]
33. Namadurai, S.; Balasuriya, D.; Rajappa, R.; Wiemhofer, M.; Stott, K.; Klingauf, J.; Edwardson, J.M.; Chirgadze, D.Y.; Jackson, A.P. Crystal structure and molecular imaging of the Nav channel beta3 subunit indicates a trimeric assembly. *J. Biol. Chem.* **2014**, *289*, 10797–10811. [[CrossRef](#)] [[PubMed](#)]
34. Ratcliffe, C.F.; Westenbroek, R.E.; Curtis, R.; Catterall, W.A. Sodium channel beta1 and beta3 subunits associate with neurofascin through their extracellular immunoglobulin-like domain. *J. Cell Biol.* **2001**, *154*, 427–434. [[CrossRef](#)]
35. Shimizu, H.; Miyazaki, H.; Ohsawa, N.; Shoji, S.; Ishizuka-Katsura, Y.; Tosaki, A.; Oyama, F.; Terada, T.; Sakamoto, K.; Shirouzu, M.; et al. Structure-based site-directed photo-crosslinking analyses of multimeric cell-adhesive interactions of voltage-gated sodium channel beta subunits. *Sci. Rep.* **2016**, *6*, 26618. [[CrossRef](#)]
36. Isom, L.L. The role of sodium channels in cell adhesion. *Front. Biosci.* **2002**, *7*, 12–23. [[CrossRef](#)]
37. Manring, H.R.; Dorn, L.E.; Ex-Willey, A.; Accornero, F.; Ackermann, M.A. At the heart of inter- and intracellular signaling: The intercalated disc. *Biophys. Rev.* **2018**, *10*, 961–971. [[CrossRef](#)]
38. Li, Y.; Merkel, C.D.; Zeng, X.; Heier, J.A.; Cantrell, P.S.; Sun, M.; Stolz, D.B.; Watkins, S.C.; Yates, N.A.; Kwiatkowski, A.V. The N-cadherin interactome in primary cardiomyocytes as defined using quantitative proximity proteomics. *J. Cell Sci.* **2019**, *132*. [[CrossRef](#)]
39. Schinner, C.; Erber, B.M.; Yeruva, S.; Waschke, J. Regulation of cardiac myocyte cohesion and gap junctions via desmosomal adhesion. *Acta Physiol.* **2019**, *226*, e13242. [[CrossRef](#)]
40. Kleber, A.G.; Saffitz, J.E. Role of the intercalated disc in cardiac propagation and arrhythmogenesis. *Front. Physiol.* **2014**, *5*, 404. [[CrossRef](#)]
41. Vozzi, C.; Dupont, E.; Coppen, S.R.; Yeh, H.I.; Severs, N.J. Chamber-related differences in connexin expression in the human heart. *J. Mol. Cell Cardiol.* **1999**, *31*, 991–1003. [[CrossRef](#)] [[PubMed](#)]
42. Goodenough, D.A.; Goliger, J.A.; Paul, D.L. Connexins, connexons, and intercellular communication. *Annu. Rev. Biochem.* **1996**, *65*, 475–502. [[CrossRef](#)] [[PubMed](#)]
43. Goldberg, G.S.; Valiunas, V.; Brink, P.R. Selective permeability of gap junction channels. *Biochim. Biophys. Acta* **2004**, *1662*, 96–101. [[CrossRef](#)]
44. Zhang, Q.; Bai, X.; Liu, Y.; Wang, K.; Shen, B.; Sun, X. Current Concepts and Perspectives on Connexin43: A Mini Review. *Curr. Protein Pept. Sci.* **2018**, *19*, 1049–1057. [[CrossRef](#)]
45. Kleber, A.G.; Rudy, Y. Basic mechanisms of cardiac impulse propagation and associated arrhythmias. *Physiol. Rev.* **2004**, *84*, 431–488. [[CrossRef](#)] [[PubMed](#)]
46. Rohr, S. Role of gap junctions in the propagation of the cardiac action potential. *Cardiovasc. Res.* **2004**, *62*, 309–322. [[CrossRef](#)]
47. Rhatt, J.M.; Veeraraghavan, R.; Poelzing, S.; Gourdie, R.G. The perinexus: Sign-post on the path to a new model of cardiac conduction? *Trends Cardiovasc. Med.* **2013**, *23*, 222–228. [[CrossRef](#)]
48. Rhatt, J.M.; Gourdie, R.G. The perinexus: A new feature of Cx43 gap junction organization. *Heart Rhythm.* **2012**, *9*, 619–623. [[CrossRef](#)]
49. Rhatt, J.M.; Ongstad, E.L.; Jourdan, J.; Gourdie, R.G. Cx43 associates with Na(v)1.5 in the cardiomyocyte perinexus. *J. Membr. Biol.* **2012**, *245*, 411–422. [[CrossRef](#)]
50. Hunter, A.W.; Barker, R.J.; Zhu, C.; Gourdie, R.G. Zonula occludens-1 alters connexin43 gap junction size and organization by influencing channel accretion. *Mol. Biol. Cell* **2005**, *16*, 5686–5698. [[CrossRef](#)]
51. Meadows, L.S.; Isom, L.L. Sodium channels as macromolecular complexes: Implications for inherited arrhythmia syndromes. *Cardiovasc. Res.* **2005**, *67*, 448–458. [[CrossRef](#)] [[PubMed](#)]
52. Sorgen, P.L.; Trease, A.J.; Spagnol, G.; Delmar, M.; Nielsen, M.S. Protein(-)Protein Interactions with Connexin 43: Regulation and Function. *Int. J. Mol. Sci.* **2018**, *19*, 1428. [[CrossRef](#)] [[PubMed](#)]
53. Makara, M.A.; Curran, J.; Little, S.C.; Musa, H.; Polina, I.; Smith, S.A.; Wright, P.J.; Unudurthi, S.D.; Snyder, J.; Bennett, V.; et al. Ankyrin-G coordinates intercalated disc signaling platform to regulate cardiac excitability In Vivo. *Circ. Res.* **2014**, *115*, 929–938. [[CrossRef](#)] [[PubMed](#)]
54. Clatot, J.; Hoshi, M.; Wan, X.; Liu, H.; Jain, A.; Shinlapawittayatorn, K.; Marionneau, C.; Ficker, E.; Ha, T.; Deschenes, I. Voltage-gated sodium channels assemble and gate as dimers. *Nat. Commun.* **2017**, *8*, 2077. [[CrossRef](#)]

55. Mori, Y.; Fishman, G.I.; Peskin, C.S. Ephaptic conduction in a cardiac strand model with 3D electrodiffusion. *Proc. Natl. Acad. Sci. USA* **2008**, *105*, 6463–6468. [[CrossRef](#)]
56. Lin, J.; Keener, J.P. Modeling electrical activity of myocardial cells incorporating the effects of ephaptic coupling. *Proc. Natl. Acad. Sci. USA* **2010**, *107*, 20935–20940. [[CrossRef](#)]
57. Hichri, E.; Abriel, H.; Kucera, J.P. Distribution of cardiac sodium channels in clusters potentiates ephaptic interactions in the intercalated disc. *J. Physiol.* **2018**, *596*, 563–589. [[CrossRef](#)]
58. Sperelakis, N. An electric field mechanism for transmission of excitation between myocardial cells. *Circ. Res.* **2002**, *91*, 985–987. [[CrossRef](#)] [[PubMed](#)]
59. Veeraghavan, R.; Lin, J.; Keener, J.P.; Gourdie, R.; Poelzing, S. Potassium channels in the Cx43 gap junction perinexus modulate ephaptic coupling: An experimental and modeling study. *Pflug. Arch.* **2016**, *468*, 1651–1661. [[CrossRef](#)]
60. Willis, B.C.; Ponce-Balbuena, D.; Jalife, J. Protein assemblies of sodium and inward rectifier potassium channels control cardiac excitability and arrhythmogenesis. *Am. J. Physiol. Heart Circ. Physiol.* **2015**, *308*, H1463–H1473. [[CrossRef](#)]
61. Abriel, H.; Rougier, J.S.; Jalife, J. Ion channel macromolecular complexes in cardiomyocytes: Roles in sudden cardiac death. *Circ. Res.* **2015**, *116*, 1971–1988. [[CrossRef](#)] [[PubMed](#)]
62. Milstein, M.L.; Musa, H.; Balbuena, D.P.; Anumonwo, J.M.; Auerbach, D.S.; Furspan, P.B.; Hou, L.; Hu, B.; Schumacher, S.M.; Vaidyanathan, R.; et al. Dynamic reciprocity of sodium and potassium channel expression in a macromolecular complex controls cardiac excitability and arrhythmia. *Proc. Natl. Acad. Sci. USA* **2012**, *109*, E2134–E2143. [[CrossRef](#)] [[PubMed](#)]
63. Lopatin, A.N.; Nichols, C.G. Inward rectifiers in the heart: An update on I(K1). *J. Mol. Cell Cardiol.* **2001**, *33*, 625–638. [[CrossRef](#)] [[PubMed](#)]
64. Burstein, B.; Nattel, S. Atrial fibrosis: Mechanisms and clinical relevance in atrial fibrillation. *J. Am. Coll. Cardiol.* **2008**, *51*, 802–809. [[CrossRef](#)] [[PubMed](#)]
65. Jeevaratnam, K.; Poh Tee, S.; Zhang, Y.; Rewbury, R.; Guzadhur, L.; Duehmke, R.; Grace, A.A.; Lei, M.; Huang, C.L. Delayed conduction and its implications in murine Scn5a(+/-) hearts: Independent and interacting effects of genotype, age, and sex. *Pflug. Arch.* **2011**, *461*, 29–44. [[CrossRef](#)]
66. Veeraghavan, R.; Hoeker, G.S.; Alvarez-Laviada, A.; Hoagland, D.; Wan, X.; King, D.R.; Sanchez-Alonso, J.; Chen, C.; Jourdan, J.; Isom, L.L.; et al. The adhesion function of the sodium channel beta subunit (beta1) contributes to cardiac action potential propagation. *eLife* **2018**, *7*. [[CrossRef](#)]
67. Malhotra, J.D.; Kazen-Gillespie, K.; Hortsch, M.; Isom, L.L. Sodium channel beta subunits mediate homophilic cell adhesion and recruit ankyrin to points of cell-cell contact. *J. Biol. Chem.* **2000**, *275*, 11383–11388. [[CrossRef](#)]
68. Raisch, T.B.; Yanoff, M.S.; Larsen, T.R.; Farooqui, M.A.; King, D.R.; Veeraghavan, R.; Gourdie, R.G.; Baker, J.W.; Arnold, W.S.; AlMahameed, S.T.; et al. Intercalated Disk Extracellular Nanodomain Expansion in Patients With Atrial Fibrillation. *Front. Physiol.* **2018**, *9*, 398. [[CrossRef](#)]
69. Watanabe, H.; Koopmann, T.T.; Le Scouarnec, S.; Yang, T.; Ingram, C.R.; Schott, J.J.; Demolombe, S.; Probst, V.; Anselme, F.; Escande, D.; et al. Sodium channel beta1 subunit mutations associated with Brugada syndrome and cardiac conduction disease in humans. *J. Clin. Investig.* **2008**, *118*, 2260–2268. [[CrossRef](#)]
70. Watanabe, H.; Darbar, D.; Kaiser, D.W.; Jiramongkolchai, K.; Chopra, S.; Donahue, B.S.; Kannankeril, P.J.; Roden, D.M. Mutations in sodium channel beta1- and beta2-subunits associated with atrial fibrillation. *Circ. Arrhythm Electrophysiol.* **2009**, *2*, 268–275. [[CrossRef](#)]
71. Kobirumaki-Shimozawa, F.; Nakanishi, T.; Shimozawa, T.; Terui, T.; Oyama, K.; Li, J.; Louch, W.E.; Ishiwata, S.; Fukuda, N. Real-Time In Vivo Imaging of Mouse Left Ventricle Reveals Fluctuating Movements of the Intercalated Discs. *Nanomaterials* **2020**, *10*, 532. [[CrossRef](#)] [[PubMed](#)]
72. Malhotra, J.D.; Koopmann, M.C.; Kazen-Gillespie, K.A.; Fettman, N.; Hortsch, M.; Isom, L.L. Structural requirements for interaction of sodium channel beta 1 subunits with ankyrin. *J. Biol. Chem.* **2002**, *277*, 26681–26688. [[CrossRef](#)] [[PubMed](#)]
73. Brackenbury, W.J.; Djamgoz, M.B.; Isom, L.L. An emerging role for voltage-gated Na⁺ channels in cellular migration: Regulation of central nervous system development and potentiation of invasive cancers. *Neuroscientist* **2008**, *14*, 571–583. [[CrossRef](#)] [[PubMed](#)]
74. Malhotra, J.D.; Thyagarajan, V.; Chen, C.; Isom, L.L. Tyrosine-phosphorylated and nonphosphorylated sodium channel beta1 subunits are differentially localized in cardiac myocytes. *J. Biol. Chem.* **2004**, *279*, 40748–40754. [[CrossRef](#)]

75. Hu, D.; Barajas-Martinez, H.; Medeiros-Domingo, A.; Crotti, L.; Veltmann, C.; Schimpf, R.; Urrutia, J.; Alday, A.; Casis, O.; Pfeiffer, R.; et al. A novel rare variant in SCN1Bb linked to Brugada syndrome and SIDS by combined modulation of Na(v)1.5 and K(v)4.3 channel currents. *Heart Rhythm*. **2012**, *9*, 760–769. [[CrossRef](#)]
76. Yereddi, N.R.; Cusdin, F.S.; Namadurai, S.; Packman, L.C.; Monie, T.P.; Slavny, P.; Clare, J.J.; Powell, A.J.; Jackson, A.P. The immunoglobulin domain of the sodium channel beta3 subunit contains a surface-localized disulfide bond that is required for homophilic binding. *FASEB J.* **2013**, *27*, 568–580. [[CrossRef](#)]
77. McEwen, D.P.; Chen, C.; Meadows, L.S.; Lopez-Santiago, L.; Isom, L.L. The voltage-gated Na⁺ channel beta3 subunit does not mediate trans homophilic cell adhesion or associate with the cell adhesion molecule contactin. *Neurosci. Lett.* **2009**, *462*, 272–275. [[CrossRef](#)]
78. Dhar Malhotra, J.; Chen, C.; Rivolta, I.; Abriel, H.; Malhotra, R.; Mattei, L.N.; Brosius, F.C.; Kass, R.S.; Isom, L.L. Characterization of sodium channel alpha- and beta-subunits in rat and mouse cardiac myocytes. *Circulation* **2001**, *103*, 1303–1310. [[CrossRef](#)]
79. Shimizu, H.; Tosaki, A.; Ohsawa, N.; Ishizuka-Katsura, Y.; Shoji, S.; Miyazaki, H.; Oyama, F.; Terada, T.; Shirouzu, M.; Sekine, S.I.; et al. Parallel homodimer structures of the extracellular domains of the voltage-gated sodium channel beta4 subunit explain its role in cell-cell adhesion. *J. Biol. Chem.* **2017**, *292*, 13428–13440. [[CrossRef](#)]
80. Shapiro, L.; Fannon, A.M.; Kwong, P.D.; Thompson, A.; Lehmann, M.S.; Grubel, G.; Legrand, J.F.; Als-Nielsen, J.; Colman, D.R.; Hendrickson, W.A. Structural basis of cell-cell adhesion by cadherins. *Nature* **1995**, *374*, 327–337. [[CrossRef](#)]
81. Harrison, O.J.; Brasch, J.; Lasso, G.; Katsamba, P.S.; Ahlsen, G.; Honig, B.; Shapiro, L. Structural basis of adhesive binding by desmocollins and desmogleins. *Proc. Natl. Acad. Sci. USA* **2016**, *113*, 7160–7165. [[CrossRef](#)] [[PubMed](#)]
82. Brasch, J.; Harrison, O.J.; Honig, B.; Shapiro, L. Thinking outside the cell: How cadherins drive adhesion. *Trends Cell Biol.* **2012**, *22*, 299–310. [[CrossRef](#)]
83. Medeiros-Domingo, A.; Kaku, T.; Tester, D.J.; Iturralde-Torres, P.; Itty, A.; Ye, B.; Valdivia, C.; Ueda, K.; Canizales-Quinteros, S.; Tusie-Luna, M.T.; et al. SCN4B-encoded sodium channel beta4 subunit in congenital long-QT syndrome. *Circulation* **2007**, *116*, 134–142. [[CrossRef](#)] [[PubMed](#)]
84. Yarbrough, T.L.; Lu, T.; Lee, H.C.; Shibata, E.F. Localization of cardiac sodium channels in caveolin-rich membrane domains: Regulation of sodium current amplitude. *Circ. Res.* **2002**, *90*, 443–449. [[CrossRef](#)] [[PubMed](#)]
85. Maguy, A.; Hebert, T.E.; Nattel, S. Involvement of lipid rafts and caveolae in cardiac ion channel function. *Cardiovasc. Res.* **2006**, *69*, 798–807. [[CrossRef](#)] [[PubMed](#)]
86. Sanon, V.P.; Sawaki, D.; Mjaatvedt, C.H.; Jourdan-Le Saux, C. Myocardial tissue caveolae. *Compr. Physiol.* **2015**, *5*, 871–886. [[CrossRef](#)]
87. Aicart-Ramos, C.; Valero, R.A.; Rodriguez-Crespo, I. Protein palmitoylation and subcellular trafficking. *Biochim. Biophys. Acta* **2011**, *1808*, 2981–2994. [[CrossRef](#)]
88. Bouza, A.A.; Philippe, J.M.; Edokobi, N.; Pinsky, A.M.; Offord, J.; Calhoun, J.D.; Lopez-Floran, M.; Lopez-Santiago, L.F.; Jenkins, P.M.; Isom, L.L. Sodium channel beta1 subunits are post-translationally modified by tyrosine phosphorylation, S-palmitoylation, and regulated intramembrane proteolysis. *J. Biol. Chem.* **2020**. [[CrossRef](#)]
89. Alday, A.; Urrutia, J.; Gallego, M.; Casis, O. alpha1-adrenoceptors regulate only the caveolae-located subpopulation of cardiac K(V)4 channels. *Channels (Austin)* **2010**, *4*, 168–178. [[CrossRef](#)]
90. Vaidyanathan, R.; Reilly, L.; Eckhardt, L.L. Caveolin-3 Microdomain: Arrhythmia Implications for Potassium Inward Rectifier and Cardiac Sodium Channel. *Front. Physiol.* **2018**, *9*, 1548. [[CrossRef](#)]
91. Marionneau, C.; Carrasquillo, Y.; Norris, A.J.; Townsend, R.R.; Isom, L.L.; Link, A.J.; Nerbonne, J.M. The sodium channel accessory subunit Navbeta1 regulates neuronal excitability through modulation of repolarizing voltage-gated K(+) channels. *J. Neurosci.* **2012**, *32*, 5716–5727. [[CrossRef](#)] [[PubMed](#)]
92. Dabiri, B.E.; Lee, H.; Parker, K.K. A potential role for integrin signaling in mechano-electrical feedback. *Prog. Biophys. Mol. Biol.* **2012**, *110*, 196–203. [[CrossRef](#)] [[PubMed](#)]
93. Kawabe, J.; Okumura, S.; Lee, M.C.; Sadoshima, J.; Ishikawa, Y. Translocation of caveolin regulates stretch-induced ERK activity in vascular smooth muscle cells. *Am. J. Physiol. Heart Circ. Physiol.* **2004**, *286*, H1845–H1852. [[CrossRef](#)]

94. Israeli-Rosenberg, S.; Chen, C.; Li, R.; Deussen, D.N.; Niesman, I.R.; Okada, H.; Patel, H.H.; Roth, D.M.; Ross, R.S. Caveolin modulates integrin function and mechanical activation in the cardiomyocyte. *FASEB J.* **2015**, *29*, 374–384. [[CrossRef](#)] [[PubMed](#)]
95. Davis, M.J.; Wu, X.; Nurkiewicz, T.R.; Kawasaki, J.; Gui, P.; Hill, M.A.; Wilson, E. Regulation of ion channels by integrins. *Cell Biochem. Biophys.* **2002**, *36*, 41–66. [[CrossRef](#)]
96. Tyan, L.; Foell, J.D.; Vincent, K.P.; Woon, M.T.; Mesquitta, W.T.; Lang, D.; Best, J.M.; Ackerman, M.J.; McCulloch, A.D.; Glukhov, A.V.; et al. Long QT syndrome caveolin-3 mutations differentially modulate Kv 4 and Cav 1.2 channels to contribute to action potential prolongation. *J. Physiol.* **2019**, *597*, 1531–1551. [[CrossRef](#)] [[PubMed](#)]
97. Vatta, M.; Ackerman, M.J.; Ye, B.; Makielski, J.C.; Ughanze, E.E.; Taylor, E.W.; Tester, D.J.; Balijepalli, R.C.; Foell, J.D.; Li, Z.; et al. Mutant caveolin-3 induces persistent late sodium current and is associated with long-QT syndrome. *Circulation* **2006**, *114*, 2104–2112. [[CrossRef](#)]
98. Echarri, A.; Del Pozo, M.A. Caveolae—mechanosensitive membrane invaginations linked to actin filaments. *J. Cell Sci.* **2015**, *128*, 2747–2758. [[CrossRef](#)]
99. Kohl, P.; Cooper, P.J.; Holloway, H. Effects of acute ventricular volume manipulation on In Situ cardiomyocyte cell membrane configuration. *Prog. Biophys. Mol. Biol.* **2003**, *82*, 221–227. [[CrossRef](#)]
100. Sinha, B.; Koster, D.; Ruez, R.; Gonnord, P.; Bastiani, M.; Abankwa, D.; Stan, R.V.; Butler-Browne, G.; Vedio, B.; Johannes, L.; et al. Cells respond to mechanical stress by rapid disassembly of caveolae. *Cell* **2011**, *144*, 402–413. [[CrossRef](#)]
101. Wary, K.K.; Mariotti, A.; Zurzolo, C.; Giancotti, F.G. A requirement for caveolin-1 and associated kinase Fyn in integrin signaling and anchorage-dependent cell growth. *Cell* **1998**, *94*, 625–634. [[CrossRef](#)]
102. Ahern, C.A.; Zhang, J.F.; Wookalis, M.J.; Horn, R. Modulation of the cardiac sodium channel Nav1.5 by Fyn, a Src family tyrosine kinase. *Circ. Res.* **2005**, *96*, 991–998. [[CrossRef](#)]
103. Beyder, A.; Rae, J.L.; Bernard, C.; Strege, P.R.; Sachs, F.; Farrugia, G. Mechanosensitivity of Nav1.5, a voltage-sensitive sodium channel. *J. Physiol.* **2010**, *588*, 4969–4985. [[CrossRef](#)] [[PubMed](#)]
104. Morris, C.E.; Juranka, P.F. Nav channel mechanosensitivity: Activation and inactivation accelerate reversibly with stretch. *Biophys. J.* **2007**, *93*, 822–833. [[CrossRef](#)]
105. Maroni, M.; Korner, J.; Schuttler, J.; Winner, B.; Lampert, A.; Eberhardt, E. beta1 and beta3 subunits amplify mechanosensitivity of the cardiac voltage-gated sodium channel Nav1.5. *Pflug. Arch.* **2019**, *471*, 1481–1492. [[CrossRef](#)] [[PubMed](#)]
106. Koivumaki, J.T.; Clark, R.B.; Belke, D.; Kondo, C.; Fedak, P.W.; Maleckar, M.M.; Giles, W.R. Na(+) current expression in human atrial myofibroblasts: Identity and functional roles. *Front. Physiol.* **2014**, *5*, 275. [[CrossRef](#)] [[PubMed](#)]
107. Nattel, S. Electrical coupling between cardiomyocytes and fibroblasts: Experimental testing of a challenging and important concept. *Cardiovasc. Res.* **2018**, *114*, 349–352. [[CrossRef](#)] [[PubMed](#)]
108. Rog-Zielinska, E.A.; Kong, C.H.T.; Zgierski-Johnston, C.M.; Verkade, P.; Mantell, J.; Cannell, M.B.; Kohl, P. Species differences in the morphology of transverse tubule openings in cardiomyocytes. *Europace* **2018**, *20*, iii120–iii124. [[CrossRef](#)]
109. Kostin, S.; Scholz, D.; Shimada, T.; Maeno, Y.; Mollnau, H.; Hein, S.; Schaper, J. The internal and external protein scaffold of the T-tubular system in cardiomyocytes. *Cell Tissue Res.* **1998**, *294*, 449–460. [[CrossRef](#)]
110. Lin, X.; O'Malley, H.; Chen, C.; Auerbach, D.; Foster, M.; Shekhar, A.; Zhang, M.; Coetzee, W.; Jalife, J.; Fishman, G.I.; et al. Scn1b deletion leads to increased tetrodotoxin-sensitive sodium current, altered intracellular calcium homeostasis and arrhythmias in murine hearts. *J. Physiol.* **2015**, *593*, 1389–1407. [[CrossRef](#)]
111. Abriel, H. Cardiac sodium channel Na(v)1.5 and interacting proteins: Physiology and pathophysiology. *J. Mol. Cell Cardiol.* **2010**, *48*, 2–11. [[CrossRef](#)] [[PubMed](#)]
112. Kitazawa, M.; Kubo, Y.; Nakajo, K. The stoichiometry and biophysical properties of the Kv4 potassium channel complex with K+ channel-interacting protein (KChIP) subunits are variable, depending on the relative expression level. *J. Biol. Chem.* **2014**, *289*, 17597–17609. [[CrossRef](#)] [[PubMed](#)]
113. Doolittle, R.F. The multiplicity of domains in proteins. *Annu. Rev. Biochem.* **1995**, *64*, 287–314. [[CrossRef](#)] [[PubMed](#)]
114. Zhao, Z.J.; Zhao, R. Purification and cloning of PZR, a binding protein and putative physiological substrate of tyrosine phosphatase SHP-2. *J. Biol. Chem.* **1998**, *273*, 29367–29372. [[CrossRef](#)]

115. Wang, L.; Nomura, Y.; Du, Y.; Dong, K. Differential effects of TipE and a TipE-homologous protein on modulation of gating properties of sodium channels from *Drosophila melanogaster*. *PLoS ONE* **2013**, *8*, e67551. [[CrossRef](#)]
116. Muhamed, I.; Chowdhury, F.; Maruthamuthu, V. Biophysical Tools to Study Cellular Mechanotransduction. *Bioengineering* **2017**, *4*, 12. [[CrossRef](#)]
117. Ohtsubo, K.; Marth, J.D. Glycosylation in cellular mechanisms of health and disease. *Cell* **2006**, *126*, 855–867. [[CrossRef](#)]
118. Cortada, E.; Brugada, R.; Verges, M. N-Glycosylation of the voltage-gated sodium channel beta2 subunit is required for efficient trafficking of NaV1.5/beta2 to the plasma membrane. *J. Biol. Chem.* **2019**, *294*, 16123–16140. [[CrossRef](#)]
119. Johnson, D.; Montpetit, M.L.; Stocker, P.J.; Bennett, E.S. The sialic acid component of the beta1 subunit modulates voltage-gated sodium channel function. *J. Biol. Chem.* **2004**, *279*, 44303–44310. [[CrossRef](#)]
120. Veeraraghavan, R.; Gourdie, R.G.; Poelzing, S. Mechanisms of cardiac conduction: A history of revisions. *Am. J. Physiol. Heart Circ. Physiol.* **2014**, *306*, H619–H627. [[CrossRef](#)]
121. Scheffer, I.E.; Harkin, L.A.; Grinton, B.E.; Dibbens, L.M.; Turner, S.J.; Zielinski, M.A.; Xu, R.; Jackson, G.; Adams, J.; Connellan, M.; et al. Temporal lobe epilepsy and GEFS+ phenotypes associated with SCN1B mutations. *Brain* **2007**, *130*, 100–109. [[CrossRef](#)] [[PubMed](#)]
122. Wang, P.; Wang, S.C.; Li, D.; Li, T.; Yang, H.P.; Wang, L.; Wang, Y.F.; Parpura, V. Role of Connexin 36 in Autoregulation of Oxytocin Neuronal Activity in Rat Supraoptic Nucleus. *ASN Neuro.* **2019**, *11*, 1759091419843762. [[CrossRef](#)] [[PubMed](#)]
123. Micevych, P.E.; Popper, P.; Hatton, G.I. Connexin 32 mRNA levels in the rat supraoptic nucleus: Up-regulation prior to parturition and during lactation. *Neuroendocrinology* **1996**, *63*, 39–45. [[CrossRef](#)] [[PubMed](#)]
124. Furshpan, E.J.; Furukawa, T. Intracellular and extracellular responses of the several regions of the Mauthner cell of the goldfish. *J. Neurophysiol.* **1962**, *25*, 732–771. [[CrossRef](#)]
125. Ter Keurs, H.E.; Zhang, Y.M.; Davidoff, A.W.; Boyden, P.A.; Wakayama, Y.; Miura, M. Damage induced arrhythmias: Mechanisms and implications. *Can. J. Physiol. Pharmacol.* **2001**, *79*, 73–81. [[CrossRef](#)]
126. Brackenbury, W.J.; Isom, L.L. Voltage-gated Na⁺ channels: Potential for beta subunits as therapeutic targets. *Expert Opin. Ther. Targets* **2008**, *12*, 1191–1203. [[CrossRef](#)]



© 2020 by the authors. Licensee MDPI, Basel, Switzerland. This article is an open access article distributed under the terms and conditions of the Creative Commons Attribution (CC BY) license (<http://creativecommons.org/licenses/by/4.0/>).